Are We Fragmented Yet?
Measuring Geopolitical Fragmentation and its Causal Effects*

Jesús Fernández-Villaverde† Tomohide Mineyama‡ Dongho Song§

University of Pennsylvania, CEPR, NBER International Monetary Fund Johns Hopkins University

March 19, 2024

Abstract

After decades of rising global economic integration, the world economy is fragmenting. To measure this phenomenon, we introduce an index of geopolitical fragmentation distilled from diverse empirical indicators. To do so, we rely on the use of a flexible, dynamic factor model with time-varying parameters and stochastic volatility. Then, we employ structural vector autoregressions and local projections to gauge the causal effects of changes in fragmentation. We show that more fragmentation impacts the global economy detrimentally but harms emerging economies more than advanced ones. We also document a key asymmetry: fragmentation immediately harms the global economy, while reduced fragmentation only unfolds gradually. A sectoral analysis within OECD economies highlights the adverse effects on those industries intricately linked to global markets, including manufacturing, construction, finance, wholesale, and retail trade.

JEL Classification: C11, C33, E00, F01, F2, F4, F6

Keywords: Dynamic factor model, causality, geopolitical fragmentation, fragmentation index

*The views expressed herein are those of the authors and should not be attributed to the IMF, its Executive Board, or its management.

†Fernández-Villaverde: jesusfv@econ.upenn.edu

‡Mineyama: TMineyama@imf.org

§Song: dongho.song@jhu.edu

1 Introduction

After decades of rising global economic integration, the world economy shifted direction in the mid-2010s. Brexit, the US-China trade war, the COVID-19 pandemic, Russia's invasion of Ukraine, and the Gaza-Israel conflict, among other events, have strained international relations and have forced many policymakers to rethink the future of their nations' economic strategies. Just as an example, the number of trade-restricting measures implemented in 2022 has nearly tripled compared to the figures recorded in 2019. Similarly, firms are re-evaluating how they operate in a context of increasing geopolitical and trade complexities. See, for more detailed discussions of this geopolitical fragmentation and its impact on the world economy, Aiyar et al. (2023a) and Gopinath (2023).

Discernible trends in geopolitical fragmentation are evident across various indicators: a global deceleration in the flows of goods and capital, increased trade and foreign direct investment restrictions, heightened political risks, more frequent sanctions, more conflicts, tighter capital controls, and growing concerns related to migration. However, none of these measures of geopolitical fragmentation summarizes the current state of world economic integration. Indeed, to the best of our knowledge, there is currently no existing comprehensive index capable of capturing the nuanced nature of geopolitical fragmentation. But without such a comprehensive index, it is hard, for instance, to perform a causal analysis of how fragmentation affects aggregate and sectoral variables or how it moves the trade-offs faced by economic policy.

In this paper, we fill this gap in the literature by creating a geopolitical fragmentation index that distills the common dynamics from a varied array of empirical indicators. Our motivating idea is that, while each indicator is inherently imperfect and is contaminated by idiosyncratic noise, there is a common dynamics behind each of the phenomena mentioned above. We extract such common dynamics with a dynamic factor model with time-varying parameters and stochastic volatility. Not only is this fully data-driven likelihood-based approach extremely flexible, but it is also capable of accommodating missing observations and handling data with different frequencies. Our principal aim is to establish an index designed for broad usage, serving the needs of politicians, practitioners, and academics alike.

Our estimated index shows three phases. First, there was a period of relative stability in geopolitical fragmentation from 1975 to the early 1990s. The fragmentation fell as the collapse of the Soviet Union and the era of market-oriented reforms across many countries led to a spike in globalization. But, in the aftermath of the Great Financial Crisis, geopolitical fragmentation has increased to the highest levels in the sample and without any indication of reversal. Our estimation results are broadly in line with the narrative approaches that have discussed the evolution of geopolitical fragmentation based on the qualitative reading of the evidence (e.g., Gopinath, 2023).

Beyond offering a quantitative assessment of the degree of geopolitical fragmentation, a key advantage of building a geopolitical fragmentation index is that we can use it as an input for standard causality analysis exercises in time series: structural vector autoregressions (SVARs) and linear projections (LPs). Our analysis reveals that a positive one-standard-deviation shock to the fragmentation index (considered adverse) has a detrimental impact on the global economy, with more pronounced negative effects observed in emerging economies compared to advanced economies. The impacts reveal asymmetry: fragmentation has an immediate negative effect on the global economy, while the positive effects of reduced fragmentation (considered as a positive aspect of globalization) unfold with lags. Our findings remain robust when defining fragmentation shock through differencing or considering various control variables, aligning with the approach taken by Caldara and Iacoviello (2022).

To elucidate the economic channels through which the economy is influenced, we specifically scrutinize sectors within OECD economies, chosen mainly because of data availability. The sectoral analysis accentuates adverse effects on those intricately connected to global markets, including manufacturing, construction, finance, wholesale, and retail trade, among others. Conversely, sectors like agriculture, forestry, fishing, real estate, and public services, which are more insulated from global markets, experience marginal effects. This sectoral pattern is particularly evident in the case of the US economy.

Our paper contributes to the expanding literature on geopolitical fragmentation, building on the summaries provided by Aiyar et al. (2023a) and Gopinath (2023). It sheds light on the associated costs, which involve the unwinding of gains from globalization, encompassing trade (e.g., Frankel and Romer, 1999, and Feenstra, 2006), technology diffusion and adoption (e.g., Bustos, 2011, and Acemoglu et al., 2015), cross-border labor and capital flows (e.g., Glennon, 2024, and Erten et al., 2021), and international risk sharing (e.g., Obstfeld, 1994).

Geopolitical tensions further contribute to increased uncertainty regarding future policies and the ultimate shape of a fragmented world (e.g., Caldara et al., 2020). The direct costs of trade disruptions include tariffs, inefficiencies from reduced specialization, resource misallocation, diminished economies of scale, and decreased competition (e.g., Melitz and Trefler, 2012). Aiyar et al. (2023a) point out that short-term transition costs stemming from trade disruptions tend to be more pronounced due to the low elasticities of substitution in the short run. In contrast, losses from technological decoupling may materialize over the medium and long term.

Moreover, the impact of these costs may vary across countries. As highlighted by Aiyar et al. (2023a), geoeconomic fragmentation disproportionately affects emerging markets and low-income countries that have the potential for catch-up through trade, financial, and technological integration. Gopinath (2023) adds that if disruptions occur primarily between large blocs (e.g., a US-Europe bloc and a China-Russia bloc), some countries, particularly in Latin America or Southeast Asia, may experience gains as "neutral" bystanders.

Given the multiple channels of impact and potential heterogeneity described above, the examination of the cost of fragmentation is an empirical question. The literature has investigated the economic consequences of recent fragmentation episodes, such as Brexit (e.g., Sampson, 2017, and Bloom et al., 2019) and the US-China trade war in 2018-19 (Fajgelbaum and Khandelwal, 2022, review the corresponding literature).

For instance, concerning the 2018 US import tariff hikes, Amiti et al. (2020) report that the increased tariffs are passed through to domestic prices, imposing their direct costs ultimately on consumers. Flaaen and Pierce (2019) and Handley et al. (2020) report negative consequences for US manufacturing employment and exports due to rising import costs and retaliatory tariffs, while Fajgelbaum et al. (2019) find that the aggregate real income loss is modest after accounting for tariff revenues and gains to domestic producers. A few studies (Góes and Bekkers, 2022, Cerdeiro et al., 2021, and Bolhuis et al., 2023) develop general equilibrium international trade models to estimate the cost of fragmentation. Estimates are substantial but vary widely, ranging from around 1% to 10% of GDP, depending on the scenarios considered and modeling assumptions.

Finally, our paper contributes to the existing body of literature focused on formulating indices or metrics. This includes assessments of uncertainty (e.g., Jurado et al., 2015, and Baker et al., 2016), geopolitical risks (e.g., Caldara and Iacoviello, 2022), economic state evaluations (e.g., Aruoba et al., 2009, and Shapiro et al., 2022), investor sentiment analysis (e.g., Baker and Wurgler, 2007), corporate credit market scrutiny (e.g., Gilchrist and Zakrajšek, 2012), shadow rate investigations (e.g., Wu and Xia, 2016), and considerations of measures related to the COVID-19 pandemic as presented by Arias et al. (2023), along with disruptions in the supply chain discussed by Bai et al. (2024).

The paper's structure is as follows. In Section 2, we examine common empirical indicators of geopolitical fragmentation in the literature. Section 3 introduces a dynamic factor model (DFM), delving into its specification and estimation intricacies, and produces the geopolitical fragmentation index. Section 4 comprehensively assesses the causal impact of geopolitical fragmentation on economic consequences. Section 5 concludes.

2 Empirical Indicators of Geopolitical Fragmentation

We compile 12 indicators of geopolitical fragmentation that have been widely employed in the literature. Each of these indicators captures an aspect of the emerging trends of geopolitical fragmentation. However, none of them synthesizes all the relevant information. By combining these indicators using a likelihood-based approach, our goal is to extract a more accurate measure of geopolitical fragmentation.[1]

[1]The methodology we present in Section 3 does not depend on the choice of these 12 indicators. Our econometric approach can accommodate more or less indicators. In fact, as new indicators become available,

2.1 Data sources for geopolitical fragmentation indicators

We begin by listing each indicator and its sources:

1. The trade openness, (export+import)/GDP, from the International Financial Statistics (IFS).
2. The FDI ratio, calculated as FDI/GDP, from the IFS.
3. The financial flow ratio, (portfolio investment+other investment)/GDP, from the IFS.
4. The number of trade restrictions, from the Global Trade Alert.
5. The capital control measure, from Fernández et al. (2016).
6. The number of sanctions, from Felbermayr et al. (2020).
7. The geopolitical risk index, from Caldara and Iacoviello (2022).
8. The trade policy uncertainty, from Caldara et al. (2020).
9. The energy uncertainty, from Dang et al. (2023).
10. The migration fear index, from Bloom et al. (2015).
11. The number of international conflicts, based on the Uppsala Conflict Data Program.
12. The UN General Assembly Kappa Score: the average of each country-pair, accessible through Häge (2017)'s database.

Panel (A) of Figure 1 presents the time series plot for each indicator. We see that most of the indicators that signal fragmentation (e.g., the capital control measure or the number of sanctions) move upward at the end of the sample, while many of the indicators that measure integration (e.g., trade openness or the financial flow ratio) stagnate. Panel (B) includes informative summary statistics that encompass the nonstationarity test and pairwise correlations between each indicator and trade openness, calculated using annual aggregated data for the available sample. The main pattern is that, although we observe evidence of comovement among indicators, there is also substantial evidence of idiosyncratic behavior, a point that reinforces our motivation of aggregating all indicators into a synthetic one.

we can incorporate them into our index or use them to replace another indicator. Nonetheless, as we argue below, the 12 indicators we select are a comprehensive survey of existing measures and our estimates will be robust to excluding different subsets of them.

Figure 1: Indicators for fragmentation

(A) Time series

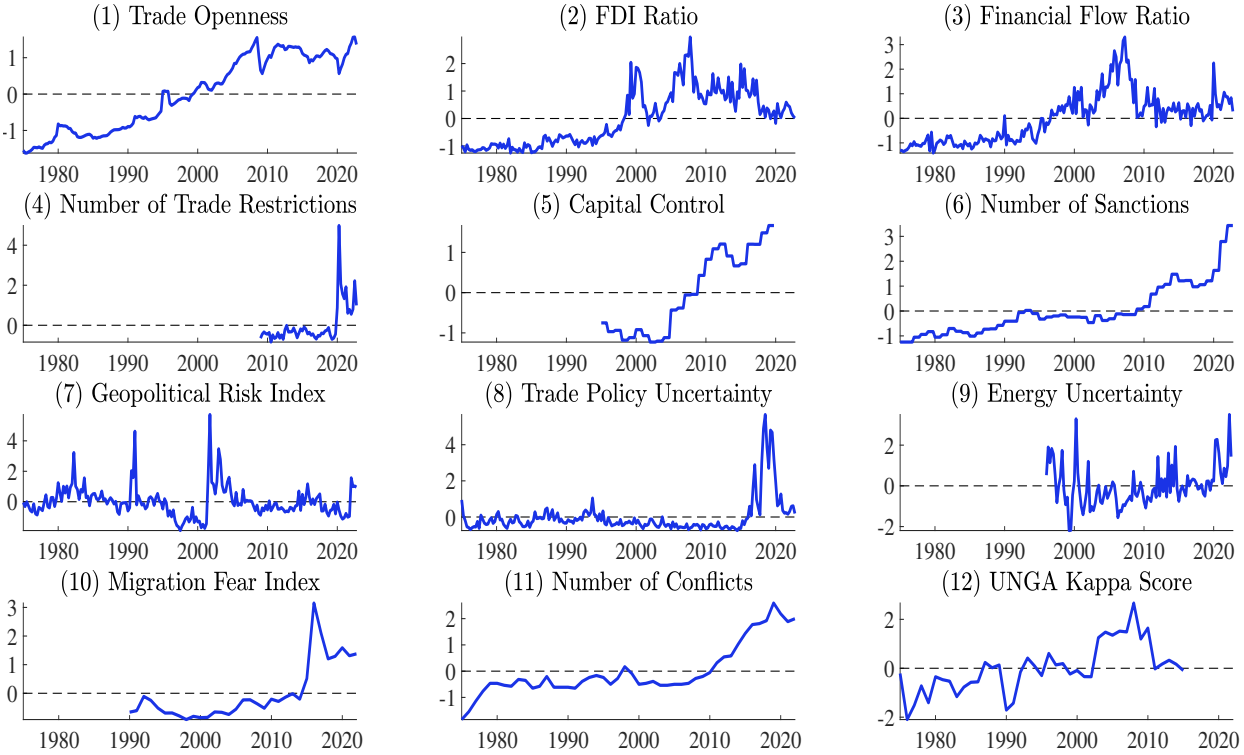

(B) Summary statistics

Category	Individual Indicators	Sample	Freq.	ADF test (p-value)	Correlation w/ Trade Openness
Trade-financial openness metrics	Trade openness	1975-2022	Q	0.32	1.00
	FDI ratio	1975-2022	Q	0.08	0.25
	Financial flow ratio	1975-2022	Q	0.07	0.33
Policy implementation gauges	Number of trade restrictions	2009-2022	Q	0.06	0.14
	Capital control measure	1980-2019	A	0.71	0.77
	Number of sanctions	1975-2022	A	1.00	0.68
Text mining-derived indicators	Geopolitical risk index	1975-2022	Q	0.00	0.03
	Trade policy uncertainty	1975-2022	Q	0.01	-0.26
	Energy uncertainty	1996-2022	Q	0.00	0.42
	Migration fear index	1990-2022	Q	0.13	0.26
Political reflections	Number of conflicts	1975-2022	Q	0.37	0.45
	UNGA Kappa score	1975-2015	A	0.01	-0.65

Notes: See main text for the sources of each indicator. All indicators are standardized to have zero mean and unit standard deviation for comparison. Indicators, except for text mining-derived ones, are the average of all countries with available data. We report the p-value derived from the Augmented Dickey-Fuller test, where the null hypothesis assumes nonstationarity.

2.2 Discussion

Next, we offer a literature review summarizing the appeal of our 12 indicators of geopolitical fragmentation and addressing associated caveats. To organize our discussion, we categorize these indicators into four areas: those measuring trade and financial openness, those gauging policy implementation, those derived from text mining, and those offering insights into political dynamics.

2.2.1 Trade and financial openness metrics

Globalization encompasses the interconnectedness and interdependence of economic and political systems worldwide. Shaped significantly by advancements facilitating the free flow of goods, services, capital, ideas, and people across national borders, its evolution is often measured through indicators such as trade openness, FDI, and financial flows relative to GDP (*indicators 1, 2, and 3*). For instance, Aiyar et al. (2023b) and Gopinath (2023) described different phases of globalization using the trade openness metric and pointed out that the remarkable increases in trade since the 1980s have stagnated since the 2008. This phenomenon is often referred to as "slowbalization." A similar deceleration is observed in FDI and financial flows. Here is an excerpt from Gopinath (2023):

> "Since 2008, however, the pace of globalization has stagnated—the so-called slowbalization—with trade to GDP stabilizing as the forces that helped spur hyperglobalization naturally waned."
>
> (IMF First Managing Deputy Director Gita Gopinath — the 20th World Congress of the International Economic Association, December 2023)

However, interpreting these dynamics requires careful consideration, as several factors, not exclusively tied to globalization or fragmentation, influence these indicators. For instance, developing countries may witness a decline in trade share due to domestic demand growth and shifts in economic structures (e.g., the expansion of non-tradable service sectors in developed countries). Moreover, economic and financial cycles play a crucial role in the dynamics of these indicators.

2.2.2 Policy implementation gauges

The dynamics of macro aggregates partly mirror underlying policy actions aimed at facilitating or impeding international flows, including the imposition or removal of trade restrictions (*indicator 4*) and capital control measures (*indicator 5*). While these policy measures directly impact fragmentation, quantifying them poses empirical challenges. Policy measures are often specific to individual countries, and their significance varies based on particular contexts. Extensive efforts in the literature have been devoted to converting qualitative information

into quantitative measures. For instance, Fernández et al. (2016) developed a quantitative measure of a country's capital control strength using diverse information, including qualitative descriptions from the IMF's Annual Report on Exchange Arrangements and Exchange Restrictions (*indicator 5*). International flow restrictions may manifest as economic sanctions, and Felbermayr et al. (2020) compiled various sanctions types, ranging from trade and financial sanctions to military assistance (*indicator 6*).

However, uncertainties persist regarding the scope of policy actions to be considered and the relevance of each measure for economic activities. Additionally, comprehensive databases may have limited time periods, constrained by the availability of consistently high-quality information over time.

2.2.3 Text mining-derived indicators

Recent advancements in text mining techniques have enabled the extraction of valuable information from extensive text data. In the realm of geopolitical fragmentation, numerous studies in the literature have crafted indices relevant to fragmentation. These encompass geopolitical events (e.g., war, terrorism, and tensions among countries and political actors) and their associated risks (Caldara and Iacoviello, 2022, *indicator 7*); uncertainty regarding trade policies (Caldara et al., 2020, *indicator 8*); energy uncertainty, often linked to geopolitical tensions (Dang et al., 2023, *indicator 9*); and concerns related to migration flows (Bloom et al., 2015, *indicator 10*). Such indices may capture the latest developments in geopolitical situations or individuals' sentiments about them, which might not be reflected in "hard" data on macroeconomic and financial activities.

2.2.4 Political reflections

Another crucial aspect of fragmentation involves political alignment, where tensions between countries can potentially escalate into violent conflicts. The Uppsala Conflict Data Program plays a pivotal role in providing a comprehensive set of conflict information based on global and local news articles (*indicator 11*). However, political misalignments often do not translate into direct actions against a country. In such instances, previous studies frequently turn to the voting behavior in the United Nations General Assembly. These studies gauge the degree of political alignment by assessing the similarity in UNGA voting patterns between countries. Häge (2017) presented derivatives of such measures, including the "kappa score," which adjusts the observed variability of countries' bilateral voting outcomes based on each country's own votes around its average vote (*indicator 12*).

2.3 Taking stock

Our previous discussion highlighted the discernible trends in geopolitical fragmentation apparent across various indicators categorized into four areas. These trends include a global deceleration in the flows of goods and capital, heightened trade and foreign direct investment restrictions, increased political risks, sanctions, and conflicts, as well as capital controls and concerns related to migration. The natural question arises: how can we quantify the dynamics of comovements within this set of empirical indicators and extract the common information present in all of them? The subsequent section addresses this issue.

3 Measuring Geopolitical Fragmentation

In the preceding section, we showed how the diverse nature of empirical indicators of geopolitical fragmentation rendered taking a simple average of them unsatisfactory. Instead, we can think about the level of geopolitical fragmentation as an unobservable variable and that each indicator is a noise measure of it. If we take this perspective, we can adopt a likelihood-based approach and let the dynamics of the indicators select the optimal weights that will yield an estimate of this unobservable variable.

More in particular, we can postulate a flexible dynamic factor model (DFM) with time-varying coefficients and stochastic volatility to account for potential parameter instability and changing uncertainty. Our approach is designed to capture the evolving comovement among time series by allowing their dependence on a common factor to change over time in flexible ways.

Factor models have been integral to the economist's toolkit over an extensive period, notably the unobservable index models proposed by Sargent and Sims (1977) and Geweke (1977). The pioneering work of Stock and Watson (1989) further solidified their significance, aiming to extract valuable information from a broad cross-section of macroeconomic time series for forecasting purposes. Our DFM description builds on the foundations of Del Negro and Otrok (2008) and Del Negro and Schorfheide (2011), utilizing Bayesian techniques for estimation, with particular emphasis on the former addressing potential parameter instability. This Bayesian methodology can be traced back to the influential works of Geweke and Zhou (1996) and Otrok and Whiteman (1998).

3.1 Specification

Let $i \in \{1, ..., N\}$ be the set of indices for the different empirical indicators of geopolitical fragmentation. In our concrete case, $N = 12$, but it could be any other finite natural number, with only the limitation of computational capabilities. The value that each indicator takes at time t is then $y_{i,t}$.

We assume that the dynamics of the $y_{i,t}$ is driven by a common factor f_t:

$$y_{i,t} = a_{i,t} + b_{i,t} f_t + u_{i,t}, \tag{1}$$

which we interpret as the true state of geopolitical fragmentation. Notice that in equation (1), the mean $a_{i,t}$, slope $b_{i,t}$, and error $u_{i,t}$ depend both on the empirical indicator and time. In that way, we incorporate much flexibility in how the factor is linked with the empirical indicators.

We assume that $a_{i,t}$ and $b_{i,t}$ evolve as:

$$\begin{aligned} a_{i,t} &= a_{i,0} + a_{i,1} t, \\ b_{i,t} &= b_{i,t-1} + \sigma_{b_i} \epsilon_{b_i,t}, \quad \epsilon_{b_i,t} \sim N(0,1). \end{aligned} \tag{2}$$

First, we address non-stationarity in the proxies $y_{i,t}$ by incorporating a deterministic time trend $a_{i,t}$ orthogonal to the common factor f_t. This is crucial, as demonstrated in Panel (B) of Figure 1, where some indicators exhibit non-stationarity while others do not. The assumption underlying our approach is that the common dynamics across empirical indicators are captured by their stationary or cyclical components. Second, we accommodate time-varying sensitivities $b_{i,t}$ of individual proxies with respect to the common factor f_t through a random-walk process, capturing potential slow-moving variations. Our goal is to allow their dependence on the factor to evolve. This flexibility is crucial, as certain indicators may reveal more about geopolitical fragmentation than others, and their importance can change dynamically over time.

In comparison, we model the evolution of the factor and the error as autoregressive processes:

$$\begin{aligned} f_t &= \phi_{f,1} f_{t-1} + ... + \phi_{f,p} f_{t-p} + \sigma_{f,t} \epsilon_{f,t}, \quad \epsilon_{f,t} \sim N(0,1), \\ u_{i,t} &= \phi_{u_i,1} u_{i,t-1} + ... + \phi_{u_i,q} u_{i,t-q} + \sigma_{u_i,t} \epsilon_{u_i,t}, \quad \epsilon_{u_i,t} \sim N(0,1). \end{aligned} \tag{3}$$

We allow the individual error terms $u_{i,t}$ to exhibit serial correlation, capturing dynamics that do not comove and are idiosyncratic to each series. This approach involves relaxing the assumption that all dynamics arise solely from the factor. The rationale behind this adjustment is to prevent the factor estimates from becoming overly dependent on a subset of empirical indicators that exhibit high persistence.

Finally, all the innovation variances, denoted by $\sigma_{k,t}$, are stochastic and display time-

varying characteristics:

$$\begin{aligned} \sigma_{k,t} &= \sigma_k \exp(h_{k,t}), \\ h_{k,t} &= h_{k,t-1} + \sigma_{h_k} \epsilon_{h_k,t}, \quad \epsilon_{h_k,t} \sim N(0,1), \quad k \in \{f, u_1, ..., u_N\}. \end{aligned} \tag{4}$$

This attribute holds for both the innovations to the common factor and those associated with the idiosyncratic error terms. The incorporation of stochastic volatility is crucial not only for modeling the non-Gaussian features inherent in the data but also for effectively capturing potential outlier events that may occur in certain years, both for the factor and the idiosyncratic terms. This dynamic approach allows the model to adapt to changing volatility patterns, offering a more robust representation of the underlying dynamics in the empirical indicators.

Compiling all the previous equations for easy reference, we get the complete specification of our DFM:

$$\begin{aligned} y_{i,t} &= a_{i,t} + b_{i,t} f_t + u_{i,t}, \\ a_{i,t} &= a_{i,0} + a_{i,1} t, \\ b_{i,t} &= b_{i,t-1} + \sigma_{b_i} \epsilon_{b_i,t}, \quad \epsilon_{b_i,t} \sim N(0,1), \\ f_t &= \phi_{f,1} f_{t-1} + ... + \phi_{f,p} f_{t-p} + \sigma_{f,t} \epsilon_{f,t}, \quad \epsilon_{f,t} \sim N(0,1), \\ u_{i,t} &= \phi_{u_i,1} u_{i,t-1} + ... + \phi_{u_i,q} u_{i,t-q} + \sigma_{u_i,t} \epsilon_{u_i,t}, \quad \epsilon_{u_i,t} \sim N(0,1), \\ \sigma_{k,t} &= \sigma_k \exp(h_{k,t}), \\ h_{k,t} &= h_{k,t-1} + \sigma_{h_k} \epsilon_{h_k,t}, \quad \epsilon_{h_k,t} \sim N(0,1), \quad k \in \{f, u_1, ..., u_N\}. \end{aligned}$$

3.2 Priors

Our priors for model parameters in (1) exhibit symmetry across a spectrum of empirical indicators related to geopolitical fragmentation $i \in \{1, ..., N\}$:

$$\begin{aligned} a_i = \begin{bmatrix} a_{i,0} \\ a_{i,1} \end{bmatrix} &\sim N\left(\begin{bmatrix} 0 \\ 0 \end{bmatrix}, \begin{bmatrix} 1 & 0 \\ 0 & \frac{1}{2} \end{bmatrix} \right), \\ \phi_k &\sim N\left(\frac{1}{2}, \frac{1}{2} \right), \\ \sigma_{b_i}^2 &\sim IG\left(1, \frac{1}{10} \right), \\ \sigma_g^2 &\sim IG\left(1, 1 \right), \end{aligned} \tag{5}$$

where $k \in \{f, u_i\}$ and $g \in \{u_i, h_f, h_{u_i}\}$.

We intentionally pick loose priors to introduce greater flexibility and reduce the sensitivity

of estimation results to the choice of prior distributions. Our priors embody the belief that the degree of time variation in the factor loading $\sigma_{b_i}^2$ is relatively smaller, approximately one-tenth, in comparison to the variations in the idiosyncratic error terms or the stochastic volatilities. However, for both cases, the weight of the prior relative to the sample for variances is not adjusted, leading to a substantial reduction in the impact of the prior as the sample length increases. We additionally explore a scenario wherein the factor loading b_i remains constant over time, and we adopt a loose prior, which is centered around one with a substantial variance of $N\left(1, \frac{1}{2}\right)$. Below, we will discuss the robustness of our results to different priors.

3.3 Estimation

The estimation procedure utilizes a Gibbs sampler to draw samples from the exact finite sample joint posterior distribution of both the parameters and the latent state variables, including the common factor. We extend the Gibbs sampler initially proposed by Del Negro and Otrok (2008), focusing on addressing the challenges associated with handling missing data and discrepancies in data frequencies, specifically pertaining to stock variables rather than flow variables. Appendix A presents a comprehensive description of the modifications we introduce.

In terms of concrete specification, we set the lag order for f_t and $u_{i,t}$ to be one, and we pick the time frame for our 12 indicators to be from 1975:Q1 to 2022:Q4. We also standardized them to have zero sample mean and unit standard deviation. The purpose of this standardization is to ensure that all the indicators contribute to the measurement of geopolitical fragmentation comparably. Trade openness, the FDI ratio, and the financial flow ratio undergo an adjustment by multiplication with -1 to account for their inverse correlation with the underlying object of interest. This adjustment facilitates the imposition of symmetric priors for factor loading across the various empirical indicators.

In instances where data is only accessible on an annual basis, the variables are characterized as stock rather than flow variables. These variables capture values at distinct points in time, akin to a snapshot or picture of the economy at that specific moment. Unlike flow variables, which depict quantities over a duration, the treatment of missing observations in this context is straightforward, as discussed in Aruoba et al. (2009). For the annual series, we assume that the individual error terms associated with them are not serially correlated.

In equation (1), there exist three sets of latent states: f_t, $b_{i,t}$, and $h_{k,t}$. All of these necessitate initialization or normalization. To mitigate the indeterminacy concerning sign and magnitude for factor loadings $b_{i,t}$ and factor levels f_t, we initialize the values for $b_{i,0}$ to one. The initialization values for f_0 and $h_{k,0}$ are set to zero, with the specific value for f_0 being non-crucial. In addition, we set the variance of innovation to the common factor to one, denoted as $\sigma_f = 1$. A more comprehensive discussion on the identification of a dynamic

factor model with time-varying loadings and stochastic volatilities can be found in Del Negro and Otrok (2008).

3.4 Results

In Figure 2, we display the posterior median (smoothed) estimates of f_t, our geopolitical fragmentation index, alongside 90% credible intervals. To aid interpretation, we overlay major historical events influencing globalization. For space efficiency, the posterior estimates for the remaining unknowns in the model can be found in Appendix C.1. As shown in Figure 1, certain indicators were unavailable until the mid-1990s, leading to wider credible intervals up to that period. We recognize the caveats in the estimation results, particularly the heightened sensitivity to empirical indicators during the initial periods from 1975 to 1995, which becomes less concerning post-1995.

Figure 2: Estimated fragmentation index

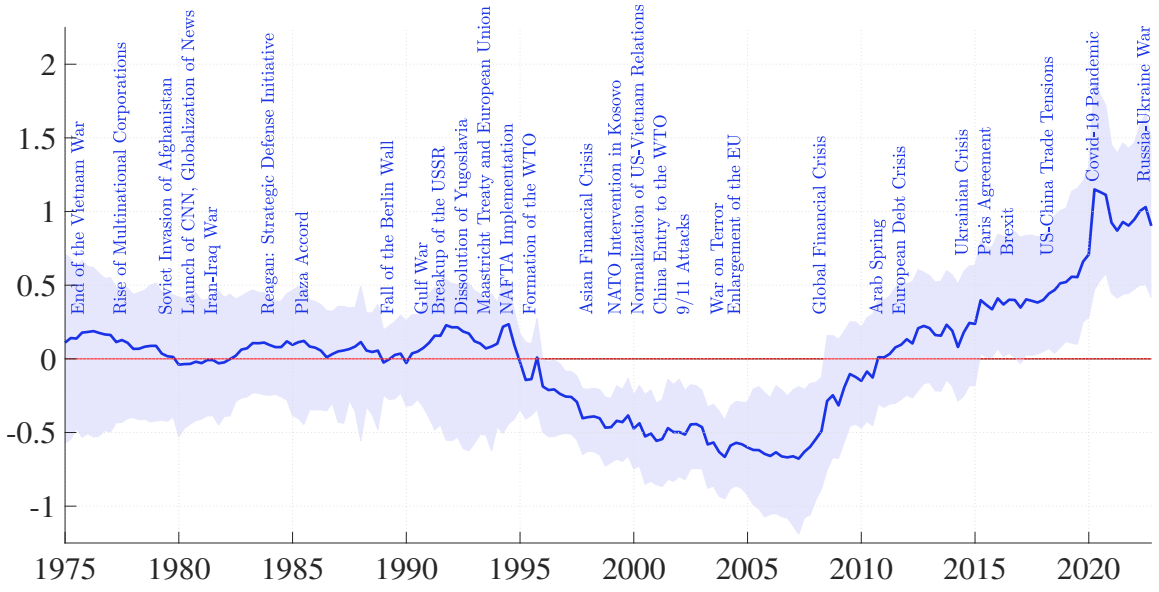

Notes: We present the posterior median-smoothed estimates of f_t accompanied by 90% credible intervals. We overlay with major historical events.

Our estimated fragmentation index aligns well with the narrative understanding of geopolitical fragmentation, as noted in Gopinath (2023). Our median estimate of fragmentation was stable between 1975 and the early 1990s. While trade openness was increasing, the world economy was still divided between the market economies and socialist economies blocs. Other indicators, like the FDI ratio or the financial flow rate, did not show much of an upward trend.

Starting from the mid-1990s, our index reports a consistent decline in fragmentation, signaling an upward trajectory in globalization. Key events contributing to this trend include the breakup of the Soviet Union, the Maastricht Treaty and the formation of the European

Union, the establishment of the World Trade Organization (WTO), and China's entry into the WTO. In fact, these were the years when the word "globalization" became popular outside of economics.

This trend shifted post-2008, experiencing a notable upswing coinciding with the Global Financial Crisis. The subsequent decade witnessed a significant surge, reflecting heightened challenges in global trade and capital flows driven by geopolitical events (e.g., conflicts, trade tensions) and the global pandemic. The process of geopolitical fragmentation has not reverted by the end of the sample (although there are some weak indications of a slowdown in fragmentation after the end of the worst phase of the COVID-19 pandemic).

3.5 Robustness checks

Next, we demonstrate the robustness of our DFM estimation results by showcasing their consistency across alternative indicator selections and prior choices.

Figure 3: Estimated fragmentation index: Alternative selection of indicators and prior choices

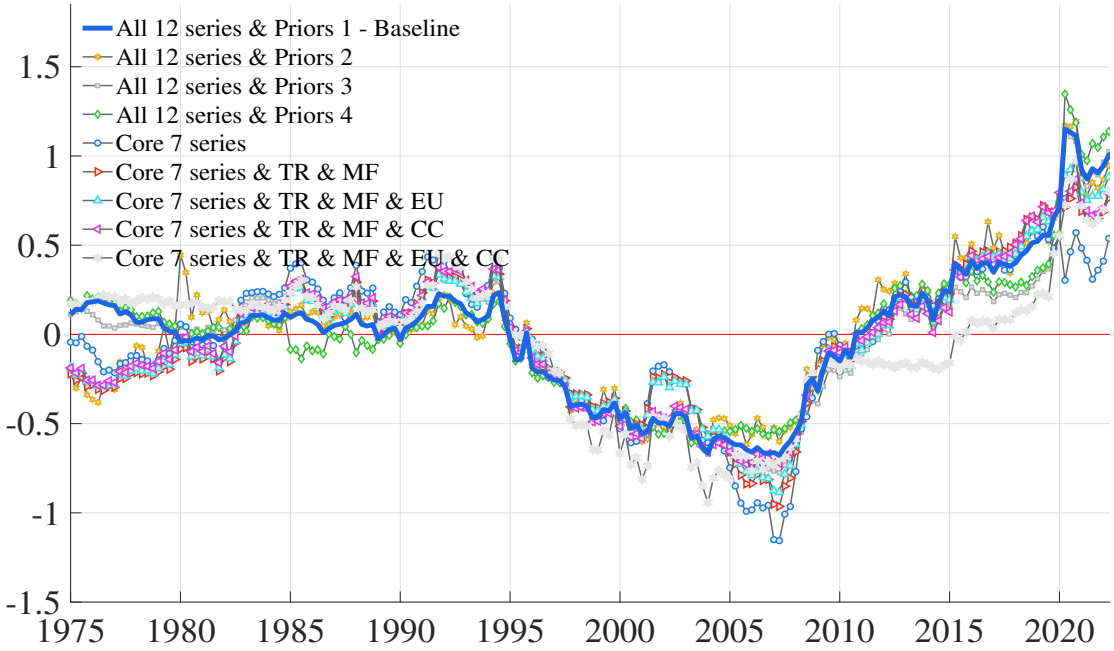

Notes: We present the median-smoothed estimate of the fragmentation index under our baseline specification, along with eight different variations.

Figure 3 plots the median estimate of our baseline specification plus a set of eight different variations. We ensure consistency by scaling all lines to match the standard deviation of the baseline case. This allows for straightforward comparison across all lines. For clarity, we designate the baseline scenario as "All 12 series & Priors 1", indicating our utilization of all

12 series of indicators in Figure 1 and adherence to the prior choices outlined in (5). Now, we explain the different lines.

First, we examine three distinct sets of prior selections for the variance parameters listed below, while preserving all 12 series. It's notable that our focus is exclusively on adjusting priors for the variance parameters, as the priors for the remaining parameters have already been set to sufficiently broad values. The rationale for organizing these choices according to their importance level is as follows. Firstly, varying options for $\sigma_{b_i}^2$ are critical as they dictate the degree of time variations in the factor loading, thereby influencing our estimation outcomes. Secondly, the priors for $\sigma_{u_i}^2$ directly impact the signal-to-noise ratio by determining the variance magnitude of the unexplained idiosyncratic component, rendering them potentially significant for estimation. Lastly, the priors for $\sigma_{h_f}^2$ and $\sigma_{h_i}^2$ regulate the extent of time variations in stochastic volatility, consequently affecting the signal-to-noise ratio. Specifically, we consider:

$$
\begin{aligned}
&\text{Priors 2:} && \sigma_{b_i}^2 \sim IG\left(10,1\right), && \sigma_{u_i}^2 \sim IG\left(10,10\right), && \sigma_{h_f}^2, \sigma_{h_i}^2 \sim IG\left(10,10\right),\\
&\text{Priors 3:} && \sigma_{b_i}^2 \sim IG\left(10,0.1\right), && \sigma_{u_i}^2 \sim IG\left(1,2\right), && \sigma_{h_f}^2, \sigma_{h_i}^2 \sim IG\left(10,1\right),\\
&\text{Priors 4:} && \sigma_{b_i}^2 \sim IG\left(10,0.1\right), && \sigma_{u_i}^2 \sim IG\left(1,0.5\right), && \sigma_{h_f}^2, \sigma_{h_i}^2 \sim IG\left(10,1\right).
\end{aligned}
$$

Subsequently, having grasped the implications of alternative prior choices on estimation outcomes, we revert to the prior choices for the baseline scenario as delineated in (5), and instead, we contemplate variations in the set of indicators. The "Core 7" denotes the scenario wherein we exclusively utilize the Trade Openness, the FDI Ratio, the Financial Flow Ratio, the Number of Sanctions, the Geopolitical Risk Index, the Trade Policy Uncertainty, and the Number of Conflicts. These indicators are termed the Core 7 owing to their quarterly frequency availability throughout the entire estimation period from 1975 to 2022. Subsequently, we incrementally incorporate (one at a time) the Number of Trade Restrictions (TR), the Migration Fear Index (MF), the Energy Uncertainty (EU), and the Capital Control (CC).

Figure 3 juxtaposes the median-smoothed estimates of the fragmentation index across these adjustments. Remarkably, the time-series plots of our estimated fragmentation index remain highly similar throughout these modifications. They consistently depict a robust correlation, averaging approximately 0.95, with the lowest observed correlation hovering around 0.86. This compelling evidence strongly reinforces our assertion that the estimation is not influenced by a specific set of empirical indicators but rather captures the authentic dynamics of fragmentation.

4 The Causal Effects of Geopolitical Fragmentation

Having estimated an index summarizing the extent of geopolitical fragmentation, we can now delve into exploring the causal link between geopolitical fragmentation and global economic activity.

Our investigation employs two widely accepted empirical techniques for causality assessment in time series: structural vector autoregressions (SVARs) and local projection (LPs). SVARs and LPs are akin in their fundamental nature, estimating dynamic relationships among observed variables within a linear projection model class, see Plagborg-Møller and Wolf (2021). In a finite sample and under model specification uncertainty, SVARs efficiently regulate the structure of relationships among variables. Conversely, LPs offer a more flexible model specification framework, exhibiting resilience against the curse of dimensionality. Their complementarities justify the use of both approaches to have a more complete assessment of the causal effects of geopolitical fragmentation.

We apply SVARs and LPs to quarterly panel data, covering a comprehensive set of macro and financial variables across a total of 60 advanced economies (AEs) and emerging markets (EMs) with available data. Descriptive statistics for these variables are provided in Appendix C.2. We begin with a panel SVAR to scrutinize the impact of fragmentation on a country's macro and financial variables. Subsequently, we transition to a panel LP analysis to explore potential heterogeneity across the sample. We complete our empirical investigation with a sectorial impact employing LPs.

4.1 Aggregate impact: A panel SVAR approach

The panel SVAR comprises 11 variables categorized into global and country components. The global block encompasses (i) our geopolitical fragmentation index, (ii) the VIX, (iii) the log of the S&P 500 index, (iv) the log of the WTI price of oil, (v) the yield on two-year U.S. Treasuries, (vi) the Chicago Federal Reserve National Financial Conditions Index (NFCI), and (vii) the log of world real GDP, aligning with the variable selection methodology of Caldara and Iacoviello (2022). These diverse global variables control for the interactions between the fragmentation index and these aggregate variables, aiding in the identification of shocks to the fragmentation index. Notably, U.S. financial market indicators are treated as "global" variables due to their influential role in the global market. The country block is comprised of (viii) the log of a country's stock price index (SP_{it}), (ix) the industrial production index (IP_{it}), (x) the log of fixed investment (I_{it}), and (xi) the log of per capita GDP (GDP_{it}).[2]

[2]For each country, we construct

$$Y'_{it} = \begin{bmatrix} \text{Fragmentation Index}_t, & \text{VIX}_t, & \ln(\text{S\&P}_t), & \ln(\text{WTI}_t), & \text{US Treasury}_t, & \text{NFCI}_t, \\ \ln(\text{World GDP}_t), & \ln(\text{SP}_{it}), & \text{IP}_{it}, & \ln(\text{I}_{it}), & \ln(\text{GDP}_{it}) & \end{bmatrix} \tag{6}$$

The SVAR incorporates two lags and utilizes quarterly data spanning from 1986:Q1 to 2022:Q4, with the starting point of the sample determined by the availability of the VIX. Data is sourced from the IMF International Financial Statistics (IFS), and observations with changes from the previous period in the top or bottom 0.5th percentile are excluded as outliers. The sample, constituting an unbalanced panel, consists of 2,359 observations from 26 countries (17 AEs and 9 EMs). The sample size is smaller than in the subsequent LP analysis since VARs necessitate the availability of all variables simultaneously. At the same time, LPs can be executed for each variable independently, resulting in more observations for regressions.

To capture country-specific factors, the panel SVAR is estimated with country-fixed effects (FEs). Standard errors are clustered by time due to the absence of cross-sectional variations in global variables. A fragmentation shock is identified through Cholesky decomposition, with the fragmentation index ordered first. This identification assumption relies on the hypothesis that geopolitical fragmentation is driven by more low-frequency forces than contemporary quarterly shocks to aggregate economic variables.

Figure 4: Economic impact of fragmentation: SVAR

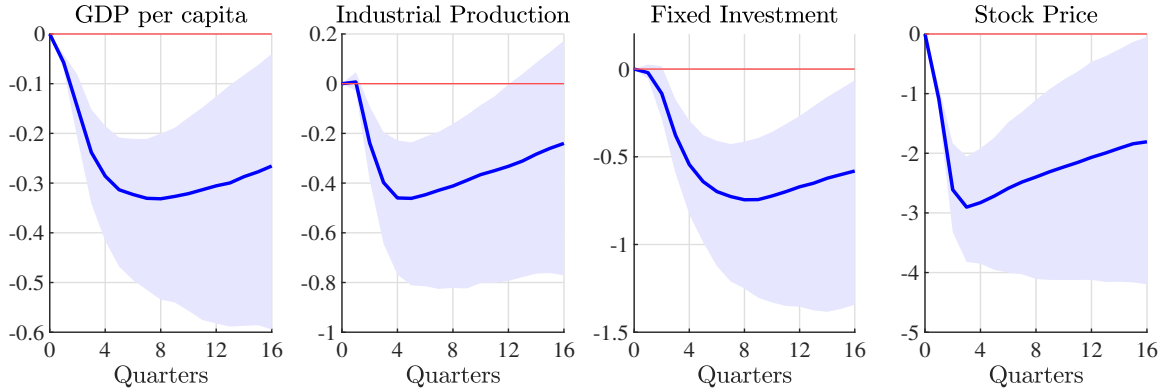

Notes: Sample of AEs and EMs. Percent responses to a one-standard-deviation fragmentation shock. Shaded areas indicate the 90th percentiles where standard errors are clustered by time.

Figure 4 presents the impulse response functions (IRFs) of country variables to a one-standard-deviation fragmentation shock. Given the assumption of identical coefficients in the VAR system across countries, these IRFs can be interpreted as the average effects of a fragmentation shock within the sample. Following a positive innovation to the fragmentation index (deemed adverse), all four country variables—GDP per capita, industrial production, fixed investment, and stock prices—experience declines. The negative effects become most pronounced approximately one to two years after the initial shock. The impact is substantial, with the peak effect of a one-standard-deviation fragmentation shock resulting in approximately a 0.3% decline in GDP.

for the panel VAR estimation.

While detailed robustness checks are outlined in Appendix C.3, we summarize the key findings here due to space constraints.

Our objective is to assess the robustness of our results by systematically examining various estimation modifications. Despite different prior choices or reliance on different sets of empirical indicators, the consistency in SVAR outcomes across these variations strengthens the credibility of our findings.

In addition, we investigated a scenario where trade openness serves as the sole indicator for geopolitical fragmentation, aligning with common practices in the field. Our findings reveal that adverse shocks to trade openness, indicative of increased fragmentation, indeed exert a negative impact on economic activities. Yet, this impact is markedly transitory, enduring only up to one year and displaying subsequent mean reversion. In contrast, our baseline results unveil a divergent narrative, highlighting the prolonged persistence of observed effects for an extended duration, exceeding three to four years. This suggests that our fragmentation measure presents a significantly different picture, which holds greater significance for the global economy.

4.2 Aggregate impact: A panel LP approach

A panel LP is implemented by estimating the following equation:

$$y_{i,t+h} - y_{i,t-1} = \beta^h s_t + \sum_{l=1}^{L} \alpha_l^h \Delta y_{i,t-l} + \sum_{l=1}^{L} \gamma_l^h s_{t-l} + \delta^h X_{i,t} + \mu_i^h + \epsilon_{i,t}^h, \tag{7}$$

for $h = 0, 1, 2,...$ where $y_{i,t+h}$ represents the outcome variable in country i at time $t + h$, i.e., $y_{i,t+h} = \{\ln(\text{GDP}_{it+h}), \text{IP}_{it+h}, \ln(\text{I}_{it+h}), \ln(\text{SP}_{it+h})\}$, and s_t is the fragmentation shock obtained in the SVAR. However, it is crucial to highlight the robustness of our results to alternative identification schemes, as illustrated in Appendix C.3.4. Following Montiel Olea and Plagborg-Møller (2021), we include lagged outcome and explanatory variables, $\Delta y_{i,t-l}$ and s_{t-l}, to address serial correlation, choosing a lag length of two.

In terms of regressors, $X_{i,t}$ is a vector of global and country-specific controls, encompassing the first and second lagged terms of a country's per capita GDP growth rate and the global variables used in the VAR analysis, i.e., the VIX, the S&P 500 index, the WTI oil price, the yield on two-year U.S. Treasuries, the NFCI, and world GDP. The WTI oil price and world GDP are taken as log-difference. μ_i^h denotes country FEs and $\epsilon_{i,t}^h$ is an error term. Standard errors are clustered by time, as in the SVAR.

The sequence of estimated coefficients, β^h for $h = 0, 1, 2,...$, represents the IRFs. The estimation period t extends until 2019:Q4 to ensure a consistent sample across the horizon h. We run the regression for each country variable separately. The number of observations differs across variables depending on data availability: 5,543 for GDP per capita (34 AEs

Figure 5: Economic impact of fragmentation: LP

(A) All countries

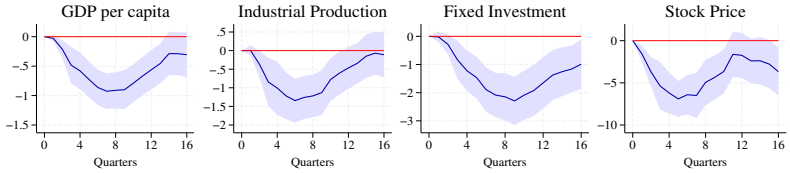

(B) AEs (**red**) versus EMs (**blue**)

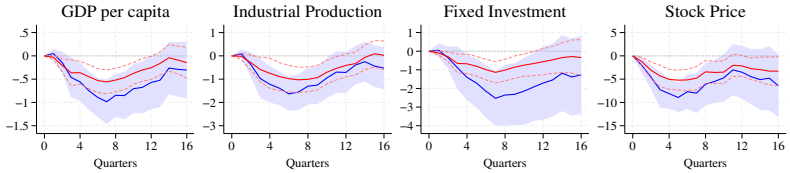

(C) West (**red**) versus East (**blue**)

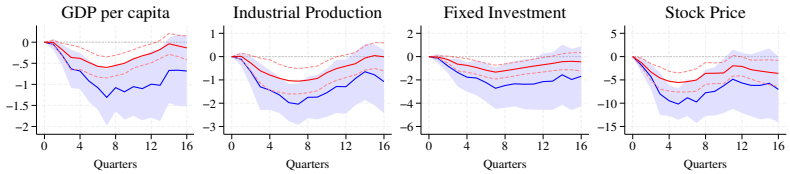

(D) High trade share (**red**) versus other countries (**blue**)

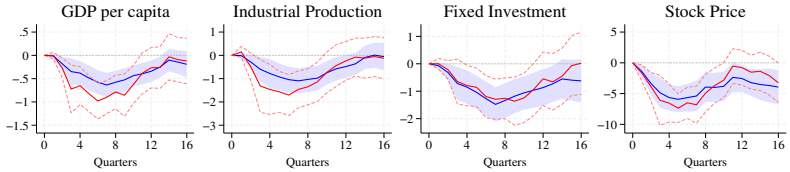

(E) High trade share with US (**red**) versus other countries (**blue**)

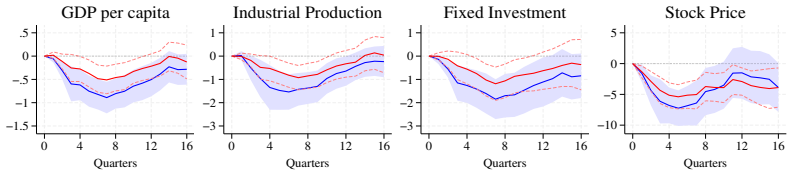

(F) Fragmentation (**red**) versus globalization (**blue**): All countries

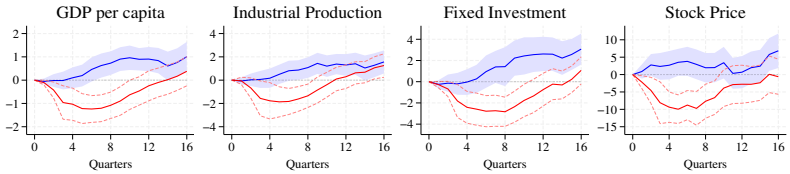

Notes: Percent responses to a 1 S.D. fragmentation shock. Shaded areas and dashed lines indicate the 90th percentiles. In Panel (A), all countries include AEs and EMs. In Panel (B), AEs and EMs follow the classification of the IMF World Economic Outlook. In Panel (C), the term "west" encompasses countries that supported the United Nations General Assembly Resolution on March 2, 2022 (ES-11/1), while "east" comprises countries that either voted against the resolution or abstained. In Panel (D), countries with trade share are defined as those with (export+import)/GDP above the median of the sample. In Panel (E), the trade share with the US is calculated using country-pair trade flows in the BACI database. In Panel (F), a positive shock to the fragmentation index is denoted as a "fragmentation" shock, while a negative shock is referred to as a "globalization" shock.

/ 27 EMs), 4,153 for industrial production, 5,010 for fixed investment, and 2,430 for stock prices in the longest horizon of the estimation ($h = 16$).

As depicted in Panel (A) of Figure 5, a fragmentation shock exhibits adverse effects on country variables, showing qualitative similarity to the SVAR result. Notably, the estimated magnitude is somewhat larger in the LP analysis; for instance, the peak response of GDP per capita is approximately 0.9%. This variance is partly attributed to the broader inclusion of emerging markets (EMs) in the sample.

In Panels (B)-(F) of Figure 5, we investigate state dependence across country and shock characteristics by incorporating distinct coefficients, thus examining variations in the regression outcomes for different countries and shocks categorized as positive versus negative:

$$y_{i,t+h} - y_{i,t-1} = \left[\mathbf{1}_{i,t-1}\beta_1^h + (1 - \mathbf{1}_{i,t-1})\beta_0^h\right] s_t + \sum_{l=1}^{L} \alpha_l^h \Delta y_{i,t-l} + \sum_{l=1}^{L} \gamma_l^h s_{t-l} + \delta^h X_{i,t} + \mu_i^h + \epsilon_{i,t}^h, \tag{8}$$

where $\mathbf{1}_{i,t}$ is an indicator variable that takes one for the sample with a specific characteristic of our interest.

In Panel (B), fragmentation has a negative impact on both AEs and EMs. Notably, the adverse repercussions are more pronounced for EMs. This suggests that countries with lower income levels experience more severe consequences from fragmentation, possibly indicating greater potential benefits from globalization.

Transitioning to Panel (C), we classify sample countries based on their voting patterns in the United Nations General Assembly Resolution on March 2, 2022, condemning Russia's aggression against Ukraine. The "East" group, comprising nations like Russia, China, India, and South Africa, which either opposed or abstained from the resolution, exhibits more substantial declines in the aftermath of a fragmentation shock.

In Panels (D) and (E), we explore the relationship between the impact of fragmentation shocks and a country's trade openness, measured by the trade share (i.e., the sum of exports and imports relative to GDP). Panel (D) highlights that nations with higher trade shares are more susceptible to the effects of fragmentation shocks. Conversely, a reversal is observed when trade openness is linked to the U.S. Countries with higher trade shares with the U.S. exhibit lower vulnerability to the impacts of fragmentation shocks, as demonstrated in Panel (E).

Lastly, Panel (F) delves into disparities between positive (fragmentation) and negative (globalization) shocks by estimating these IRFs separately in the state-dependency regression (8). This figure illustrates that fragmentation shocks exert immediate adverse impacts on the global economy, whereas the effects of globalization shocks unfold gradually over 2 to 3 years, demonstrating greater persistence.

4.3 Sectoral impact: A panel LP approach

4.3.1 OECD countries

The preceding section's analysis indicates that fragmentation has adverse effects on the overall economy. The focus now shifts to examining how fragmentation influences various sectors within a country, with a particular emphasis on OECD countries.

The OECD conducts an annual breakdown of GDP across ten major sectors, aligning closely with the 2-digit US Standard Industrial Classification (SIC) classification used in the subsequent section, covering its 38 member countries. Utilizing VAR-identified fragmentation shocks and employing the set of control variables from the preceding section, we perform a panel LP analysis of (7). The dataset, an unbalanced panel, spans from 1986 to 2022, with most countries' data becoming available only in the late 1990s.

Panel (A) of Figure 6 illustrates the IRFs to fragmentation shocks on sectoral GDP in OECD countries. Sectors with greater exposure to global economic and financial activities, such as manufacturing, construction (investment activities), wholesale & retail trade, information & communication, and professional services, demonstrate more pronounced responses. In contrast, domestically oriented sectors like agriculture & forestry & fishing, real estate, and public services exhibit muted reactions. Importantly, this discernible sectoral pattern is also observed in the case of the U.S. economy, a point we delve into in the following section.

4.3.2 United States

In this section, we explore sectoral data within the U.S. Using annual GDP data compiled by the Bureau of Economic Analysis (BEA) since 1977 (with quarterly data available from 2005:Q1 onward), we employ a panel LP approach outlined in equation (7) covering the period from 1986 to 2022. The control variables include U.S. aggregate GDP growth and the same global variables utilized in the cross-country analysis. The fragmentation shocks, aggregated annually, serve as the central variable of interest.

Panel (B) of Figure 6 illustrates the IRs of U.S. sectoral GDP to fragmentation shocks. Our focus is on the ten major private sectors and the government sector at the 2-digit level of the SIC within regional GDP. The figure highlights the concentrated adverse effects of fragmentation in specific sectors, including manufacturing, durable goods, transportation, and wholesales, likely attributed to the heightened exposure of these sectors to global economic activities.

5 Conclusions

After decades of global economic integration, recent trends point to a shift towards fragmentation. We offer a measure of geopolitical fragmentation, drawn from diverse empirical

Figure 6: Fragmentation impact on sectoral GDP

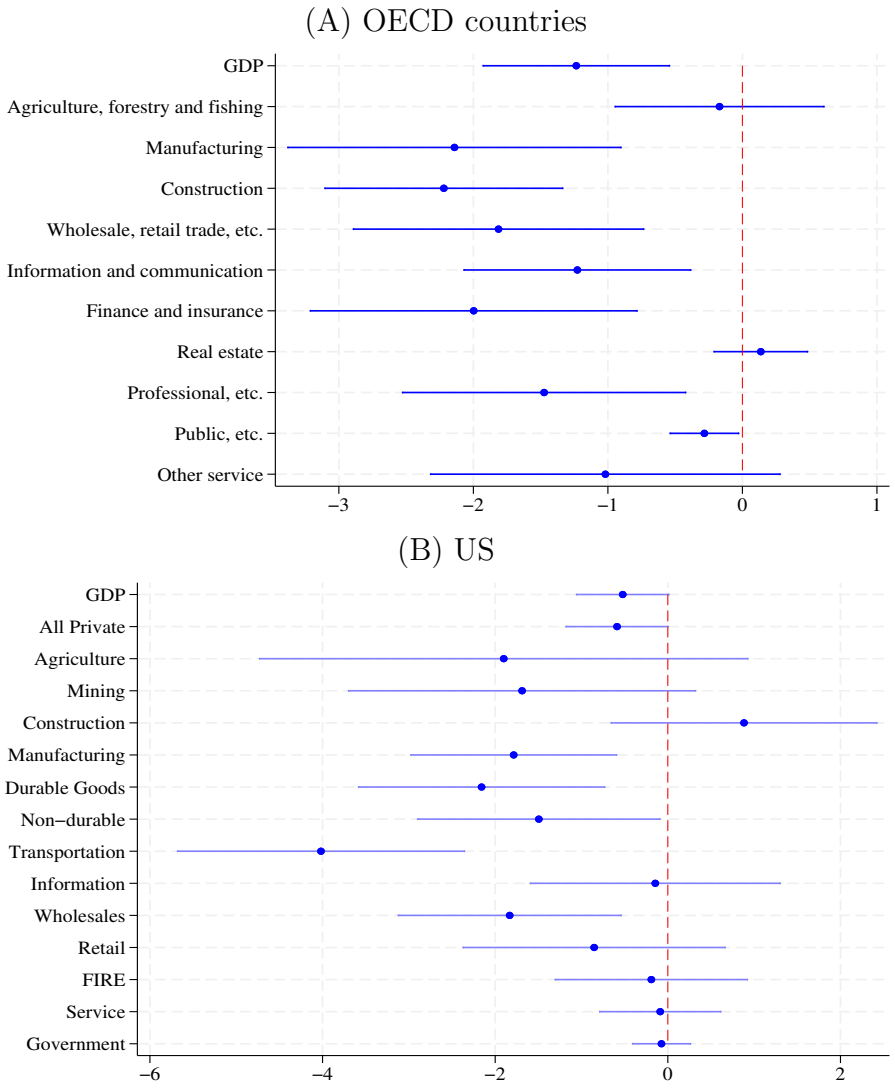

Notes: Panel (A): Sample of 38 OECD countries with sectoral breakdown. Percent responses of 1-year ahead GDP to a 1 S.D. shock to the factor. Bars indicate the 90 percentiles. "Wholesale, retail trade, etc." includes wholesale, retail trade, repairs, transport, accommodation, and food services. "Professional, etc." represents professional, scientific, and support services. "Public, etc." is the sum of public administration, defense, education, health, and social work. Panel (B): Sample of 8 BEA regions with sectoral breakdown. Percent responses of 1-year ahead GDP to a 1 S.D. shock to the factor. Bars indicate the 90 percentiles. Since the BEA stopped updating GDP by state before 1997, we map the previous SIC to the current NAICS. Specifically, the SIC "communications" sector is connected to "information" under the NAICS; the SIC "service" is to the sum of "professional and business services", "management of companies and enterprises," "educational service, health care, and social assistance," and "arts, entertainment, recreation, accommodation, and food services"; other sectors are connected to the sectors with the same labels in the SIC and the NAICS.

indicators, to precisely assess the current state and contribute to understanding its causal effects on the global economy. Leveraging a widely-used method extended for maximum flexibility, our estimated dynamic factor model with time-varying parameters and stochastic volatility captures the evolving dynamics of global fragmentation.

Our analysis, employing SVAR and LP, reveals the causal relationships between changes in fragmentation and their impacts on the global economy. We find that heightened fragmentation, indicated by a positive one-standard-deviation shock to the fragmentation index, detrimentally affects the global economy, with emerging economies disproportionately affected compared to advanced ones. Importantly, we uncover an inherent asymmetry: while fragmentation immediately impairs the global economy, the benefits of reduced fragmentation, often associated with positive aspects of globalization, unfold gradually over time. Additionally, our examination of sectors within OECD economies highlights the adverse repercussions of fragmentation on industries intricately connected to global markets, including manufacturing, construction, finance, wholesale, and retail trade.

References

Acemoglu, D., Gancia, G., and Zilibotti, F. (2015). Offshoring and directed technical change. *American Economic Journal: Macroeconomics*, 7:84–122.

Aiyar, S., Chen, J., Ebeke, C., Ebeke, C. H., Garcia-Saltos, R., Gudmundsson, T., Ilyina, A., Kangur, A., Kunaratskul, T., Rodriguez, M. S. L., et al. (2023a). *Geo-economic fragmentation and the future of multilateralism*. International Monetary Fund.

Aiyar, S., Presbitero, A., and Ruta, M. (2023b). *Geoeconomic Fragmentation: The Economic Risks from a Fractured World Economy*. CEPR Press.

Amiti, M., Redding, S. J., and Weinstein, D. E. (2020). Who's paying for the us tariffs? a longer-term perspective. *AEA Papers and Proceedings*, 110:541–546.

Arias, J. E., Fernández-Villaverde, J., Rubio-Ramírez, J. F., and Shin, M. (2023). The causal effects of lockdown policies on health and macroeconomic outcomes. *American Economic Journal: Macroeconomics*, 15(3):287–319.

Aruoba, S. B., Diebold, F. X., and Scotti, C. (2009). Real-time measurement of business conditions. *Journal of Business and Economic Statistics*, 27(4):417–427.

Bai, X., Fernández-Villaverde, J., Li, Y., and Zanetti, F. (2024). The causal effects of global supply chain disruptions on macroeconomic outcomes: Evidence and theory. Manuscript.

Baker, M. and Wurgler, J. (2007). Investor sentiment in the stock market. *Journal of Economic Perspectives*, 21(2):129–152.

Baker, S. R., Bloom, N., and Davis, S. J. (2016). Measuring Economic Policy Uncertainty. *Quarterly Journal of Economics*, 131(4):1593–1636.

Bloom, N., Bunn, P., Chen, S., Mizen, P., Smietanka, P., and Thwaites, G. (2019). The impact of brexit on uk firms. NBER Working Paper No. 26218.

Bloom, N., Davis, S., and Baker, S. (2015). Immigration fears and policy uncertainty. VOXEU Column, 15 December, 2015.

Bolhuis, M. A., Chen, J., and Kett, B. (2023). Fragmentation in global trade: Accounting for commodities. IMF Working Paper WP/23/73, International Monetary Fund.

Bustos, P. (2011). Trade liberalization, exports, and technology upgrading: Evidence on the impact of mercosur on argentinian firms. *American Economic Review*, 101:304–340.

Caldara, D. and Iacoviello, M. (2022). Measuring geopolitical risk. *American Economic Review*, 112(4):1194–1225.

Caldara, D., Iacoviello, M., Molligo, P., Prestipino, A., and Raffo, A. (2020). The economic effects of trade policy uncertainty. *Journal of Monetary Economics*, 109:38–59.

Carter, C. K. and Kohn, R. (1994). On Gibbs sampling for state space models. *Biometrika*, 81(3):541–553.

Cerdeiro, D. A., Eugster, J., Mano, R. C., Muir, D., and Peiris, S. J. (2021). Sizing up the effects of technological decoupling. IMF Working Paper, WP/21/69.

Dang, T. H.-N., Nguyen, C. P., Lee, G. S., Nguyen, B. Q., and Le, T. T. (2023). Measuring the energy-related uncertainty index. *Energy Economics*, 124(106817).

Del Negro, M. and Otrok, C. (2008). Dynamic factor models with time-varying parameters: Measuring changes in international business cycles. *Federal Reserve Bank of New York Staff Reports no. 326*.

Del Negro, M. and Schorfheide, F. (2011). Bayesian macroeconometrics. In Geweke, J., Koop, G., and van Dijk, H., editors, *The Oxford Handbook of Bayesian Econometrics*, pages 293–389. Oxford University Press.

Durbin, J. and Koopman, S. J. (2001). *Time Series Analysis by State Space Methods*. Oxford University Press.

Erten, B., Korinek, A., and Ocampo, J. A. (2021). Capital controls: Theory and evidence. *Journal of Economic Literature*, 59(1):45–89.

Fajgelbaum, P. D., Goldberg, P. K., Kennedy, P. J., and Khandelwal, A. K. (2019). Return to protectionism. *Quarterly Journal of Economics*, 135:1–55.

Fajgelbaum, P. D. and Khandelwal, A. K. (2022). The economic impacts of the us–china trade war. *Annual Review of Economics*, 14:205–228.

Feenstra, R. C. (2006). New evidence on the gains from trade. *Review of World Economics / Weltwirtschaftliches Archiv*, 142(4):617–641.

Felbermayr, G., Kirilakha, A., Syropoulos, C., Yalcin, E., and Yotov, Y. V. (2020). The global sanctions data base. *European Economic Review*, 129:103561.

Fernández, A., Klein, M. W., Rebucci, A., Schindler, M., and Uribe, M. (2016). Capital control measures: A new dataset. *IMF Economic Review*, 64:548–574.

Flaaen, A. and Pierce, J. (2019). Disentangling the effects of the 2018-2019 tariffs on a globally connected u.s. manufacturing sector. Finance and Economics Discussion Series 2019-086, Federal Reserve Board.

Frankel, J. A. and Romer, D. H. (1999). Does trade cause growth? *American Economic Review*, 89(3):379–399.

Geweke, J. (1977). The dynamic factor analysis of economic time series. In Aigner, D. J. and Goldberger, A. S., editors, *Latent Variables in Socio-Economic Models*, chapter 19. North Holland, Amsterdam.

Geweke, J. and Zhou, G. (1996). Measuring the pricing error of the arbitrage pricing theory. *Review of Financial Studies*, 9(2):557–587.

Gilchrist, S. and Zakrajšek, E. (2012). Credit spreads and business cycle fluctuations. *American Economic Review*, 102(4):1692–1720.

Glennon, B. (2024). How do restrictions on high-skilled immigration affect offshoring? evidence from the h-1b program. *Management Science*, 70:907–930.

Góes, C. and Bekkers, E. (2022). The impact of geopolitical conflicts on trade, growth, and innovation. World Trade Organization, Staff Working Paper ERSD-2022-09.

Gopinath, G. (2023). Cold War II? Preserving economic cooperation amid geoeconomic fragmentation. Plenary Speech at the 20th World Congress of the International Economic Association, Colombia, December 11, 2023.

Häge, F. M. (2017). Chance-corrected measures of foreign policy similarity (fpsim version 2). Harvard Dataverse, V2.

Handley, K., Kamal, F., and Monarch, R. (2020). Rising import tariffs, falling export growth: When modern supply chains meet old-style protectionism. NBER Working Paper No. 26611.

Jurado, K., Ludvigson, S. C., and Ng, S. (2015). Measuring uncertainty. *American Economic Review*, 105(3):1177–1216.

Kim, S., Shephard, N., and Chib, S. (1998). Stochastic volatility: Likelihood inference and comparison with arch models. *Review of Economic Studies*, 65(3):361–393.

Melitz, M. J. and Trefler, D. (2012). Gains from trade when firms matter. *Journal of Economic Perspectives*, 26(2):91–118.

Montiel Olea, J. L. and Plagborg-Møller, M. (2021). Local projection inference is simpler and more robust than you think. *Econometrica*, 89(4):1789–1823.

Obstfeld, M. (1994). Risk-taking, global diversification, and growth. *American Economic Review*, 84:1310–1329.

Otrok, C. and Whiteman, C. H. (1998). Bayesian leading indicators: Measuring and predicting economic conditions in iowa. *International Economic Review*, 39(4):997–1014.

Plagborg-Møller, M. and Wolf, C. K. (2021). Local projection and vars estimate the same impulse. *Econometrica*, 89(2):955–980.

Sampson, T. (2017). Brexit: The economics of international disintegration. *Journal of Economic Perspectives*, 31:163–184.

Sargent, T. J. and Sims, C. A. (1977). Business cycle modeling without pretending to have too much a priori economic theory. In *New Methods in Business Cycle Research*. FRB Minneapolis, Minneapolis.

Shapiro, A. H., Sudhof, M., and Wilson, D. J. (2022). Measuring news sentiment. *Journal of Econometrics*, 228(2):221–243.

Stock, J. H. and Watson, M. W. (1989). New indices of coincident and leading economic indicators. In Blanchard, O. J. and Fischer, S., editors, *NBER Macroeconomics Annual 1989*, volume 4, pages 351–394. MIT Press, Cambridge.

Wu, J. C. and Xia, F. D. (2016). Measuring the macroeconomic impact of monetary policy at the zero lower bound. *Journal of Money, Credit and Banking*, 48(2-3):253–291.

Appendix

A Estimation of the Dynamic Factor Model

The dynamic factor model with time-varying parameters is specified as

$$
\begin{aligned}
y_{i,t} &= a_{i,t} + b_{i,t} f_t + u_{i,t}, \\
a_{i,t} &= a_{i,0} + a_{i,1} t, \\
f_t &= \phi_{f,1} f_{t-1} + ... + \phi_{f,p} f_{t-p} + \sigma_{f,t} \epsilon_{f,t}, \quad \epsilon_{f,t} \sim N(0,1), \\
b_{i,t} &= b_{i,t-1} + \sigma_{b_i} \epsilon_{b_i,t}, \quad \epsilon_{b_i,t} \sim N(0,1), \\
u_{i,t} &= \phi_{u_i,1} u_{i,t-1} + ... + \phi_{u_i,q} u_{i,t-q} + \sigma_{u_i,t} \epsilon_{u_i,t}, \quad \epsilon_{u_i,t} \sim N(0,1), \\
h_{j,t} &= h_{j,t-1} + \sigma_{h_j} \epsilon_{h_j,t}, \quad \sigma_{j,t} = \sigma_j \exp(h_{j,t}), \quad \epsilon_{h_j,t} \sim N(0,1),
\end{aligned}
\tag{A-1}
$$

where $i \in \{1, ..., N\}$ and $j \in \{f, u_1, ..., u_N\}$. To simplify the explanation, we gather the parameters in (A-1) as

$$
a_0 = \begin{bmatrix} a_{0,1} \\ \vdots \\ a_{0,N} \end{bmatrix}, \quad a_1 = \begin{bmatrix} a_{1,1} \\ \vdots \\ a_{1,N} \end{bmatrix}, \quad b_t = \begin{bmatrix} b_{1,t} \\ \vdots \\ b_{N,t} \end{bmatrix}, \quad \sigma_b = \begin{bmatrix} \sigma_{b_1} \\ \vdots \\ \sigma_{b_N} \end{bmatrix}, \quad \phi_f = \begin{bmatrix} \phi_{f,1} \\ \vdots \\ \phi_{f,p} \end{bmatrix},
\tag{A-2}
$$

$$
\phi_{u_i} = \begin{bmatrix} \phi_{u_i,1} \\ \vdots \\ \phi_{u_i,q} \end{bmatrix}, \quad \phi_u = \begin{bmatrix} \phi_{u_1} \\ \vdots \\ \phi_{u_N} \end{bmatrix}, \quad \sigma_u = \begin{bmatrix} \sigma_{u_1} \\ \vdots \\ \sigma_{u_N} \end{bmatrix}, \quad \sigma_{h_u} = \begin{bmatrix} \sigma_{h_{u_1}} \\ \vdots \\ \sigma_{h_{u_N}} \end{bmatrix}.
$$

The model unknowns can be categorized into three sets

$$
\Theta_f = \{f^T, \phi_f, \sigma_f, h_f^T\}, \quad \Theta_b = \{b^T, \sigma_b\}, \quad \Theta_u = \{a_0, a_1, \phi_u, \sigma_u, h_u^T\}.
$$

A.1 Gibbs sampler

We use the Gibbs sampler to estimate the model unknowns. For the k-th iteration,

(G1) Appendix A.2: Run Kalman filter and smoother using the algorithm to update $\Theta_f^{(k)}$ conditional on $\Theta_f^{(k-1)}, \Theta_b^{(k-1)}, \Theta_u^{(k-1)}$

(G2) Appendix A.3: Run Kalman filter and smoother using the algorithm to update $\Theta_b^{(k)}$ conditional on $\Theta_f^{(k)}, \Theta_b^{(k-1)}, \Theta_u^{(k-1)}$

(G3) Appendix A.4: Update the remaining parameters, including ones associated with the serially correlated innovation $\Theta_u^{(k)}$ conditional on $\Theta_f^{(k)}, \Theta_b^{(k)}, \Theta_u^{(k-1)}$

A.2 Updating the factor and the associated parameters: $\Theta_f^{(k)}$

For ease of exposition, we omit the superscript (k). We re-express (A-1) as

$$\begin{aligned}
&\tilde{y}_{i,t} = \tilde{a}_{i,t} + \tilde{b}_{i,t}\tilde{f}_t + \sigma_{u_i,t}\epsilon_{u_i,t}, \\
&\tilde{y}_{i,t} = (y_{i,t} - \phi_{u_i,1}y_{i,t-1} ... - \phi_{u_i,q}y_{i,t-q}), \\
&\tilde{a}_{i,t} = a_{i,0}(1 - \phi_{u_i,1} ... - \phi_{u_i,q}) + a_{i,1}(t - \phi_{u_i,1}(t-1) ... - \phi_{u_i,q}(t-q)), \\
&\tilde{b}_{i,t} = \begin{bmatrix} b_{i,t} & -b_{i,t-1}\phi_{u_i,1} & \dots & -b_{i,t-q}\phi_{u_i,q} \end{bmatrix}.
\end{aligned} \tag{A-3}$$

Note that (A-3) implies the following state-space representation

$$\begin{bmatrix} \tilde{y}_{1,t} \\ \vdots \\ \tilde{y}_{N,t} \end{bmatrix} = \begin{bmatrix} \tilde{a}_{1,t} \\ \vdots \\ \tilde{a}_{N,t} \end{bmatrix} + \begin{bmatrix} \tilde{b}_{1,t} \\ \vdots \\ \tilde{b}_{N,t} \end{bmatrix} \cdot \begin{bmatrix} f_t \\ f_{t-1} \\ \vdots \\ f_{t-q} \end{bmatrix} + \begin{bmatrix} \sigma_{u_1,t}\epsilon_{u_1,t} \\ \vdots \\ \sigma_{u_N,t}\epsilon_{u_N,t} \end{bmatrix}, \tag{A-4}$$

$$\begin{bmatrix} f_t \\ f_{t-1} \\ \vdots \\ f_{t-q} \end{bmatrix} = \begin{bmatrix} \phi_{f,1} & \dots & \phi_{f,p} & \dots \\ 1 & \dots & 0 & \dots \\ 0 & \ddots & \vdots & \dots \\ \dots & 0 & 1 & \dots \end{bmatrix} \begin{bmatrix} f_{t-1} \\ f_{t-2} \\ \vdots \\ f_{t-q-1} \end{bmatrix} + \begin{bmatrix} \sigma_{f,t}\epsilon_{f,t} \\ 0 \\ \vdots \\ 0 \end{bmatrix}.$$

Based on the state-space representation in (A-4), we draw f^T based on the forward filtering and backward smoothing algorithm explained in Appendix A.5. Conditional on the drawn f^T, we draw $\{\phi_f, \sigma_f, h_f^T\}$ based on the procedure described in Appendix A.6.

A.3 Updating the factor loading and the associated parameter: $\Theta_b^{(k)}$

For ease of exposition, we omit the superscript (k).

For each $i \in \{1, ..., N\}$, we re-express (A-1) as

$$
\begin{aligned}
\hat{y}_{i,t} &= \hat{a}_{i,t} + \hat{f}_t \hat{b}_{i,t} + \sigma_{u_i,t} \epsilon_{u_i,t}, \\
\hat{y}_{i,t} &= (y_{i,t} - \phi_{u_i,1} y_{i,t-1} ... - \phi_{u_i,q} y_{i,t-q}), \\
\tilde{a}_{i,t} &= a_{i,0}(1 - \phi_{u_i,1} ... - \phi_{u_i,q}) + a_{i,1}(t - \phi_{u_i,1}(t-1) ... - \phi_{u_i,q}(t-q)), \\
\hat{f}_t &= \begin{bmatrix} f_t & -f_{t-1}\phi_{u_i,1} & \dots & -f_{t-q}\phi_{u_i,q} \end{bmatrix}, \\
\hat{b}_{i,t} &= \begin{bmatrix} b_{i,t} \\ b_{i,t-1} \\ \vdots \\ b_{i,t-q} \end{bmatrix} = \begin{bmatrix} 1 & \dots & 0 & \dots \\ 1 & \dots & 0 & \dots \\ 0 & \ddots & \vdots & \dots \\ \dots & 0 & 1 & \dots \end{bmatrix} \begin{bmatrix} b_{i,t-1} \\ b_{i,t-2} \\ \vdots \\ b_{i,t-q-1} \end{bmatrix} + \begin{bmatrix} \sigma_{b_i} \epsilon_{b_i,t} \\ 0 \\ \vdots \\ 0 \end{bmatrix}.
\end{aligned}
\tag{A-5}
$$

Based on the state-space representation in (A-5), we draw b_i^T based on the forward filtering and backward smoothing algorithm explained in Appendix A.5. Conditional on the drawn b_i^T, we draw σ_{b_i} based on the procedure described in Appendix A.6.

A.4 Updating the remaining parameters: $\Theta_u^{(k)}$

For ease of exposition, we omit the superscript (k). First, conditional on $\{\phi_u, \sigma_u, h_u^T\}$, we re-express (A-1) as

$$
\bar{y}_{i,t} = a_i \bar{x}_{i,t} + \sigma_{u_i} \epsilon_{u_i,t} \tag{A-6}
$$

where

$$
\bar{y}_{i,t} = \frac{\hat{y}_{i,t} - \hat{f}_t \hat{b}_{i,t}}{\exp(h_{u_i,t})}, \quad \bar{x}_{i,t} = \begin{bmatrix} \frac{1 - \phi_{u_i,1} ... - \phi_{u_i,q}}{\exp(h_{u_i,t})}, & \frac{t - \phi_{u_i,1}(t-1) ... - \phi_{u_i,q}(t-q)}{\exp(h_{u_i,t})} \end{bmatrix},
$$

and $\hat{y}_{i,t}$, $\hat{f}_t$, and $\hat{b}_{i,t}$ are provided in (A-5). We draw a_i based on the procedure described in Appendix A.6. Second, conditional on the updated a, we re-express (A-1) as

$$
u_{i,t} = y_{i,t} - a_{i,t} - b_{i,t} f_t \tag{A-7}
$$

and update the associated parameters and stochastic volatilities $\{\phi_u, \sigma_u, h_u^T\}$ of the serially correlated errors based on the procedure described in Appendix A.6.

A.5 Forward filtering and backward smoothing algorithm

To illustrate the forward filtering and backward smoothing algorithm by Carter and Kohn (1994), we will use a generic expression for the state-space model

$$\begin{aligned} o_t &= A + Z_t s_t + \eta_t, \quad \eta_t \sim N(0, \Omega_t), \\ s_t &= \Phi s_{t-1} + \varepsilon_t, \quad \varepsilon_t \sim N(0, \Sigma_t). \end{aligned} \tag{A-8}$$

We summarized the standard Kalman filter as described in Durbin and Koopman (2001). Suppose that the distribution of

$$s_{t-1}|y^{t-1} \sim N(s_{t-1|t-1}, P_{t-1|t-1}).$$

Then, the Kalman filter forecasting and updating equations take the form

$$\begin{aligned} s_{t|t-1} &= \Phi s_{t-1|t-1} \\ P_{t|t-1} &= \Phi P_{t-1|t-1}\Phi' + \Sigma_t \\ s_{t|t} &= s_{t|t-1} + (Z_t P_{t|t-1})'(Z_t P_{t|t-1} Z_t')^{-1}\left(o_t - A - Z_t s_{t|t-1}\right) \\ P_{t|t} &= P_{t|t-1} - (Z_t P_{t|t-1})'(Z_t P_{t|t-1} Z_t')^{-1}(Z_t P_{t|t-1}). \end{aligned}$$

In turn,

$$s_t|o^t \sim N(s_{t|t}, P_{t|t}).$$

The backward smoothing algorithm developed by Carter and Kohn (1994) is applied to generate draws from the distributions $s_\tau recursively|s_{\tau+1}, ..., s_T, o^T$ (ignoring dependency on model unknowns) for $\tau = T-1, T-2, \ldots, 1$. The last elements of the Kalman filter recursion provide the initialization for the simulation smoother:

$$\begin{aligned} s_{\tau|\tau+1} &= s_{\tau|\tau} + P_{\tau|\tau}\Phi' P_{\tau+1|t}^{-1}\left(s_{\tau+1} - \Phi s_{\tau|\tau}\right) \\ P_{\tau|\tau+1} &= P_{\tau|\tau} - P_{\tau|\tau}\Phi' P_{\tau+1|\tau}^{-1}\Phi P_{\tau|\tau} \\ \text{draw } s_\tau &\sim N(s_{\tau|\tau+1}, P_{\tau|\tau+1}), \qquad \tau = T-1, T-2, ..., 1. \end{aligned}$$

A.6 Drawing persistence, variance, and stochastic volatility of the autoregressive model

To illustrate the procedure, we will use a generic expression for the autoregressive model. To simplify, we assume an AR(1) model with stochastic volatility as described in (A-9)

$$x_t = \rho_x x_{t-1} + \sigma_x \exp(h_t)\epsilon_{x,t}, \quad \epsilon_{x,t} \sim N(0,1). \tag{A-9}$$

Drawing ρ_x. In order to obtain posterior for ρ_x we assume that for $t \leq 0$, $h_t = 0$. Under this assumption x_0 is generated from a stationary distribution. Express the unconditional distribution as

$$x_0 \sim N(0, \Sigma_{x_0})$$

where $\Sigma_{x_0} = \frac{1}{(1-\rho_x^2)}$. From (A-9), we get $var(x_1) = \rho_x^2 var(x_0) + \exp(2h_1) = S_{x_0}$ where $S_{x_0} = \rho_x^2 \Sigma_{x_0} + \exp(2h_1)$. We write the conditional likelihood of the first factor element as

$$L(x_1|h_1, \rho_x) = \frac{1}{\sqrt{2\pi S_{x0}}} \exp\left\{-\frac{1}{2S_{x0}} x_1^2\right\} \tag{A-10}$$

and the remaining $T-1$ elements as

$$\begin{aligned} L(x_2, ..., x_T|h_{1:T}, \rho_x) &= \prod_{t=2}^{T} \frac{1}{\sqrt{2\pi \exp(2h_t)}} \exp\left\{-\frac{1}{2}(\frac{x_t - \rho_x x_{t-1}}{\exp(h_t)})'(\frac{x_t - \rho_x x_{t-1}}{\exp(h_t)})\right\} \\ &\propto \exp\left\{\frac{1}{2}(e_0 - E_0\rho_x)'(e_0 - E_0\rho_x)\right\} \end{aligned} \tag{A-11}$$

where

$$e_0 = \begin{bmatrix} \frac{x_2}{\exp(h_2)} \\ \vdots \\ \frac{x_T}{\exp(h_T)} \end{bmatrix}, \quad E_0 = \begin{bmatrix} \frac{x_1}{\exp(h_2)} \\ \vdots \\ \frac{x_{T-1}}{\exp(h_T)} \end{bmatrix}.$$

We use

$$\rho_x \sim N(V_{\rho_x}^{-1}(\bar{V}_{\rho_x}\bar{\rho}_x + E_0' e_0), V_{\rho_x}^{-1})$$

as a proposal distribution, where $V_{\rho_x} = \bar{V}_{\rho_x} + E_0' E_0$. In a Metropolis-Hastings step, we accept the draw ρ_x generated from the proposal distribution with probability

$$\min\left\{\frac{L(x_1|h_1, \rho_x^{(k)})}{L(x_1|h_1, \rho_x^{(k-1)})}, 1\right\}.$$

Drawing σ_x^2. The posterior for σ_x^2 is given by

$$\sigma_x^2 \sim IG\left(\frac{\bar{T}+T}{2}, \bar{v} + (e_0 - E_0\rho_x)'(e_0 - E_0\rho_x)\right).$$

Drawing h^T. The last step of the Gibbs sampler draws the stochastic volatilities conditional

Table A-1: Approximating constants: $\{q_k, m_k, r_k\}$

ι	$q_k = Pr(\iota = k)$	m_k	r_k^2
1	0.00730	-10.12999	5.79596
2	0.10556	-3.97281	2.61369
3	0.00002	-8.56686	5.17950
4	0.04395	2.77786	0.16735
5	0.34001	0.61942	0.64009
6	0.24566	1.79518	0.34023
7	0.25750	-1.08819	1.26261

on all other parameters. Define γ_t such that

$$\gamma_t = \left(\frac{x_t - \rho_x x_{t-1}}{\sigma_x} \right) = \exp(h_t)\epsilon_{x,t}.$$

Taking squares and then logs of z_t produces,

$$z_t^* = 2h_t + u_t^* \tag{A-12}$$

$$h_t = \rho_h h_{t-1} + \sigma_h \varepsilon_t. \tag{A-13}$$

where $z_t^* = log(\gamma_t^2 + 0.001)$ and $u_t^* = log(\epsilon_{x,t}^2)$. Observe that ε_t and u_t^* are not correlated. The resulting state-space representation is linear but not Gaussian since the measurement error u_t^* is distributed as a $\ln(\chi_1^2)$. We approximate $\ln(\chi_1^2)$ using a mixture of normals and transform the system into a Gaussian one following Kim et al. (1998). Express the distribution of u_t^* as

$$f(u_t^*) = \sum_{k=1}^{K} q_k f_N(u_t^* | \iota_t = k)$$

where ι_t is the indicator variable selecting which member of the mixture of normals has to be used at time t. $f_N(\cdot)$ denotes the pdf of a normal distribution, and $q_k = Pr(\iota_t = k)$. Kim et al. (1998) select a mixture of seven normals ($K = 7$) with component probabilities q_k, means $m_k - 1.2704$, and variances r_k^2.

Conditional on $\iota_{1:T}$, the system has an approximate linear and Gaussian state-space form to which the standard Kalman filtering algorithm and the backward recursion of Carter and Kohn (1994) can be applied. Drawing h^T is then straightforward. The parameters associated with h^T can be generated from the following posterior distributions

$$\begin{aligned} \rho_h &\sim N(V_{\rho_h}^{-1}(\bar{V}_{\rho_h}\bar{\rho}_h + \sigma_h^{-2} h'_{1:T-1} h_{2:T}), V_{\rho_h}^{-1}) \\ \sigma_h^2 &\sim IG(\frac{\bar{T}_h + T}{2}, \bar{v}_h + d_h^2) \end{aligned}$$

where $V_{\rho_h} = \bar{V}_{\rho_h} + \sigma_h^{-2} h'_{1:T-1} h_{1:T-1}$ and $d_h^2 = (h_{2:T} - \rho_h h_{1:T})'(h_{2:T} - \rho_h h_{1:T})$. The final task is to draw a new sample of indicators, $\iota_{1:T}$ conditional on u_t^* and h_t:

$$Pr(\iota_t = k | u_t^*, h_t) \propto q_k f_N(u_{jt}^* | 2h_t + m_k - 1.2704, r_k^2).$$

B Estimation of the Extended Dynamic Factor Model

A bloc is indexed by j (where $j \in \{1, ..., J\}$), multiple empirical indicators, denoted by $i \in \{1, ..., N\}$, exhibit a shared dynamic behavior described by the function $f_t^{(j)}$:

$$\begin{aligned}
y_{i,t}^{(j)} &= a_{i,t}^{(j)} + b_{i,t}^{(j)} f_t^{(j)} + u_{i,t}^{(j)}, \\
a_{i,t}^{(j)} &= a_{i,0}^{(j)} + a_{i,1}^{(j)} t, \\
f_t^{(j)} &= \phi_{f,1}^{(j)} f_{t-1}^{(j)} + ... + \phi_{f,p}^{(j)} f_{t-p}^{(j)} + \sigma_{f,t}^{(j)} \epsilon_{f,t}^{(j)}, \quad \epsilon_{f,t}^{(j)} \sim N(0,1), \\
b_{i,t}^{(j)} &= b_{i,t-1}^{(j)} + \sigma_{b_i}^{(j)} \epsilon_{b_i,t}^{(j)}, \quad \epsilon_{b_i,t}^{(j)} \sim N(0,1), \\
u_{i,t}^{(j)} &= \phi_{u_i,1}^{(j)} u_{i,t-1}^{(j)} + ... + \phi_{u_i,q}^{(j)} u_{i,t-q}^{(j)} + \sigma_{u_i,t}^{(j)} \epsilon_{u_i,t}^{(j)}, \quad \epsilon_{u_i,t}^{(j)} \sim N(0,1), \\
h_{k,t}^{(j)} &= h_{k,t-1}^{(j)} + \sigma_{h_k}^{(j)} \epsilon_{h_k,t}^{(j)}, \quad \sigma_{k,t}^{(j)} = \sigma_k^{(j)} \exp(h_{k,t}^{(j)}), \quad \epsilon_{h_k,t}^{(j)} \sim N(0,1), \quad k \in \{f, u_1, ..., u_N\}.
\end{aligned} \tag{A-14}$$

Variables without the superscript j signify that they are generated globally or derived from cross-bloc averages. We assume that the global factor is expressed as weighted averages of the local factors through the following equations:

$$\begin{aligned}
y_{i,t} &= a_{i,t} + b_{i,t} \left(\sum_{j=1}^{J} w_j f_t^{(j)} \right) + u_{i,t}, \\
a_{i,t} &= a_{i,0} + a_{i,1} t, \\
b_{i,t} &= b_{i,t-1} + \sigma_{b_i} \epsilon_{b_i,t}, \quad \epsilon_{b_i,t} \sim N(0,1), \\
u_{i,t} &= \phi_{u_i,1} u_{i,t-1} + ... + \phi_{u_i,q} u_{i,t-q} + \sigma_{u_i,t} \epsilon_{u_i,t}, \quad \epsilon_{u_i,t} \sim N(0,1), \\
h_{k,t} &= h_{k,t-1} + \sigma_{h_k} \epsilon_{h_k,t}, \quad \sigma_{k,t} = \sigma_k \exp(h_{k,t}), \quad \epsilon_{h_k,t} \sim N(0,1), \quad k \in \{f, u_1, ..., u_N\}.
\end{aligned} \tag{A-15}$$

For ease of exposition, we partition the model unknowns into

$$\Theta_{f-}^{(j)} = \{\phi_f^{(j)}, \sigma_f^{(j)}, h_f^{(j),T}\}, \quad \Theta_b^{(j)} = \{b^{(j),T}, \sigma_b^{(j)}\}, \quad \Theta_u^{(j)} = \{a_0^{(j)}, a_1^{(j)}, \phi_u^{(j)}, \sigma_u^{(j)}, h_u^{(j),T}\},$$

where $j \in \{1, ..., J\}$ indexes a bloc and

$$\Theta_{f+} = \{f^{(1),T}, ..., f^{(J),T}\}, \quad \Theta_w = \{w_1, ..., w_J\}, \quad \Theta_b = \{b^T, \sigma_b\}, \quad \Theta_u = \{a_0, a_1, \phi_u, \sigma_u, h_u^T\}.$$

In total, the model unknowns are summarized as follows

$$\Theta = \left\{ \Theta_{f+}, \Theta_w, \Theta_b, \Theta_u, \{\Theta_{f-}^{(j)}, \Theta_b^{(j)}, \Theta_u^{(j)}\}_{j=1}^J \right\}. \tag{A-16}$$

B.1 Modified Gibbs sampler

We adapt the Gibbs sampler to estimate the model unknowns Θ as follows. Without loss of generality, let's assume that we are at the k-th iteration.

(M1) Update $\left[\{\Theta_{f-}^{(j)}, \Theta_b^{(j)}, \Theta_u^{(j)}\}_{j=1}^J\right]^{(k+1)}$ conditional on $\Theta_{f+}^{(k)}, \Theta_w^{(k)}, \Theta_b^{(k)}, \Theta_u^{(k)}$: For each bloc $j \in \{1, ..., J\}$, we iterate through (G1), (G2), and (G3), as summarized in Appendix A.1.

(M2) Update $\Theta_b^{(k+1)}$ and $\Theta_u^{(k+1)}$ conditional on $\left[\{\Theta_{f-}^{(j)}, \Theta_b^{(j)}, \Theta_u^{(j)}\}_{j=1}^J\right]^{(k+1)}$, $\Theta_{f+}^{(k)}$, and $\Theta_w^{(k)}$: We iterate through (G2), and (G3), as summarized in Appendix A.1. At this step, when we condition on the set of local factors, the parameters and states governing local dynamics $\left[\{\Theta_{f-}^{(j)}, \Theta_b^{(j)}, \Theta_u^{(j)}\}_{j=1}^J\right]^{(k+1)}$ do not impact the update of global parameters.

(M3) Update $\Theta_{f+}^{(k+1)}$ conditional on , $\Theta_w^{(k)}, \Theta_b^{(k+1)}, \Theta_u^{(k+1)}$ and $\left[\{\Theta_{f-}^{(j)}, \Theta_b^{(j)}, \Theta_u^{(j)}\}_{j=1}^J\right]^{(k+1)}$. Appendix B.2 provides the detailed instruction.

(M4) Update $\Theta_w^{(k+1)}$ conditional on $\Theta_{f+}^{(k+1)}, \Theta_b^{(k+1)}, \Theta_u^{(k+1)}$ and $\left[\{\Theta_{f-}^{(j)}, \Theta_b^{(j)}, \Theta_u^{(j)}\}_{j=1}^J\right]^{(k+1)}$. Appendix B.3 provides the detailed instruction.

B.2 Drawing the local factors

We re-express (A-14) as

$$\begin{aligned}
\tilde{y}_{i,t}^{(j)} &= \tilde{a}_{i,t}^{(j)} + \tilde{b}_{i,t}^{(j)} \tilde{f}_t^{(j)} + \sigma_{u_i,t}^{(j)} \epsilon_{u_i,t}^{(j)}, \\
\tilde{y}_{i,t}^{(j)} &= (y_{i,t}^{(j)} - \phi_{u_i,1}^{(j)} y_{i,t-1}^{(j)} ... - \phi_{u_i,q}^{(j)} y_{i,t-q}^{(j)}), \\
\tilde{a}_{i,t}^{(j)} &= a_{i,0}^{(j)}(1 - \phi_{u_i,1}^{(j)} ... - \phi_{u_i,q}^{(j)}) + a_{i,1}^{(j)}(t - \phi_{u_i,1}^{(j)}(t-1) ... - \phi_{u_i,q}^{(j)}(t-q)), \\
\tilde{b}_{i,t}^{(j)} &= \begin{bmatrix} b_{i,t}^{(j)} & -b_{i,t-1}^{(j)} \phi_{u_i,1}^{(j)} & \dots & -b_{i,t-q}^{(j)} \phi_{u_i,q}^{(j)} \end{bmatrix}.
\end{aligned} \tag{A-17}$$

Note that (A-17) implies the following state-space representation

$$\begin{bmatrix} \tilde{y}_{1,t}^{(j)} \\ \vdots \\ \tilde{y}_{N,t}^{(j)} \end{bmatrix} = \begin{bmatrix} \tilde{a}_{1,t}^{(j)} \\ \vdots \\ \tilde{a}_{N,t}^{(j)} \end{bmatrix} + \begin{bmatrix} \tilde{b}_{1,t}^{(j)} \\ \vdots \\ \tilde{b}_{N,t}^{(j)} \end{bmatrix} \cdot \begin{bmatrix} f_t^{(j)} \\ f_{t-1}^{(j)} \\ \vdots \\ f_{t-q}^{(j)} \end{bmatrix} + \begin{bmatrix} \sigma_{u_1,t}^{(j)} \epsilon_{u_1,t}^{(j)} \\ \vdots \\ \sigma_{u_N,t}^{(j)} \epsilon_{u_N,t}^{(j)} \end{bmatrix}, \tag{A-18}$$

$$\begin{bmatrix} f_t^{(j)} \\ f_{t-1}^{(j)} \\ \vdots \\ f_{t-q}^{(j)} \end{bmatrix} = \begin{bmatrix} \phi_{f,1}^{(j)} & \dots & \phi_{f,p}^{(j)} & \dots \\ 1 & \dots & 0 & \dots \\ 0 & \ddots & \vdots & \dots \\ \dots & 0 & 1 & \dots \end{bmatrix} \begin{bmatrix} f_{t-1}^{(j)} \\ f_{t-2}^{(j)} \\ \vdots \\ f_{t-q-1}^{(j)} \end{bmatrix} + \begin{bmatrix} \sigma_{f,t}^{(j)} \epsilon_{f,t}^{(j)} \\ 0 \\ \vdots \\ 0 \end{bmatrix}.$$

For ease of illustration, we re-express the state-space representation in (A-18) as

$$\begin{aligned} \tilde{\mathbf{y}}_t^{(j)} &= \tilde{\mathbf{a}}_t^{(j)} + \tilde{\mathbf{b}}_t^{(j)} \mathbf{f}_t^{(j)} + \boldsymbol{\sigma}_{u,t}^{(j)} \odot \boldsymbol{\epsilon}_{u,t}^{(j)}, \\ \mathbf{f}_t^{(j)} &= \boldsymbol{\phi}_f^{(j)} \mathbf{f}_{t-1}^{(j)} + \boldsymbol{\sigma}_{f,t}^{(j)} \odot \boldsymbol{\epsilon}_{f,t}^{(j)}. \end{aligned} \tag{A-19}$$

The measurement equation of (A-15) can be expressed in a similar fashion as follows

$$\tilde{\mathbf{y}}_t = \tilde{\mathbf{a}}_t + \tilde{\mathbf{b}}_t \left(\sum_{j=1}^{J} w_j \mathbf{f}_t^{(j)} \right) + \boldsymbol{\sigma}_{u,t} \odot \boldsymbol{\epsilon}_{u,t}. \tag{A-20}$$

We concatenate (A-19) and (A-20) as follows

$$\begin{bmatrix} \tilde{\mathbf{y}}_t \\ \tilde{\mathbf{y}}_t^{(1)} \\ \vdots \\ \tilde{\mathbf{y}}_t^{(J)} \end{bmatrix} = \begin{bmatrix} \tilde{\mathbf{a}}_t \\ \tilde{\mathbf{a}}_t^{(1)} \\ \vdots \\ \tilde{\mathbf{a}}_t^{(J)} \end{bmatrix} + \begin{bmatrix} w_1 \tilde{\mathbf{b}}_t & w_2 \tilde{\mathbf{b}}_t & \dots & w_J \tilde{\mathbf{b}}_t \\ \tilde{\mathbf{b}}_t^{(1)} & \mathbf{0} & \dots & \mathbf{0} \\ \vdots & \vdots & \ddots & \vdots \\ \mathbf{0} & \mathbf{0} & \dots & \tilde{\mathbf{b}}_t^{(J)} \end{bmatrix} \begin{bmatrix} \mathbf{f}_t^{(1)} \\ \vdots \\ \mathbf{f}_t^{(J)} \end{bmatrix} + \begin{bmatrix} \boldsymbol{\sigma}_{u,t} \odot \boldsymbol{\epsilon}_{u,t} \\ \boldsymbol{\sigma}_{u,t}^{(1)} \odot \boldsymbol{\epsilon}_{u,t}^{(1)} \\ \vdots \\ \boldsymbol{\sigma}_{u,t}^{(J)} \odot \boldsymbol{\epsilon}_{u,t}^{(J)} \end{bmatrix}, \tag{A-21}$$

$$\begin{bmatrix} \mathbf{f}_t^{(1)} \\ \vdots \\ \mathbf{f}_t^{(J)} \end{bmatrix} = \begin{bmatrix} \boldsymbol{\phi}_f^{(1)} & \dots & \mathbf{0} \\ \vdots & \ddots & \vdots \\ \mathbf{0} & \dots & \boldsymbol{\phi}_f^{(J)} \end{bmatrix} \begin{bmatrix} \mathbf{f}_{t-1}^{(1)} \\ \vdots \\ \mathbf{f}_{t-1}^{(J)} \end{bmatrix} + \begin{bmatrix} \boldsymbol{\sigma}_{f,t}^{(1)} \odot \boldsymbol{\epsilon}_{f,t}^{(1)} \\ \vdots \\ \boldsymbol{\sigma}_{f,t}^{(J)} \odot \boldsymbol{\epsilon}_{f,t}^{(J)} \end{bmatrix}.$$

Based on the state-space representation in (A-21), we draw $[\ \mathbf{f}_t^{(1)'} \ \dots \ \mathbf{f}_t^{(J)'}\ ]$ for all $t \in \{1, ..., T\}$, i.e., Θ_{f+}, based on the forward filtering and backward smoothing algorithm explained in Appendix A.5.

B.3 Drawing the weights associated with the local factors

We re-arrange (A-20) as follows

$$\tilde{\mathbf{y}}_t - \tilde{\mathbf{a}}_t = \begin{bmatrix} \tilde{\mathbf{b}}_t \mathbf{f}_t^{(1)} & \tilde{\mathbf{b}}_t \mathbf{f}_t^{(2)} & \dots & \tilde{\mathbf{b}}_t \mathbf{f}_t^{(J)} \end{bmatrix} \begin{bmatrix} w_1 \\ w_2 \\ \vdots \\ w_J \end{bmatrix} + \boldsymbol{\sigma}_{u,t} \odot \boldsymbol{\epsilon}_{u,t}. \tag{A-22}$$

By defining

$$\begin{aligned} \widehat{\mathbf{y}}_t &\equiv \left(\tilde{\mathbf{y}}_t - \tilde{\mathbf{a}}_t\right) \oslash \boldsymbol{\sigma}_{u,t} \\ \widehat{\mathbf{x}}_t &\equiv \begin{bmatrix} \tilde{\mathbf{b}}_t \mathbf{f}_t^{(1)} \oslash \boldsymbol{\sigma}_{u,t} & \tilde{\mathbf{b}}_t \mathbf{f}_t^{(2)} \oslash \boldsymbol{\sigma}_{u,t} & \dots & \tilde{\mathbf{b}}_t \mathbf{f}_t^{(J)} \oslash \boldsymbol{\sigma}_{u,t} \end{bmatrix} \end{aligned} \tag{A-23}$$

where $A \oslash B$ means A is divided by B element-wise, we can re-express (A-22) as

$$\widehat{\mathbf{y}}_t = \widehat{\mathbf{x}}_t \mathbf{w} + \boldsymbol{\epsilon}_{u,t}. \tag{A-24}$$

We refer to Appendix A.6 for drawing $\mathbf{w}$.

C Supplementary Figures and Tables

C.1 Posterior estimates

Figure A-1: Posterior estimates: Constants, persistence, volatilities

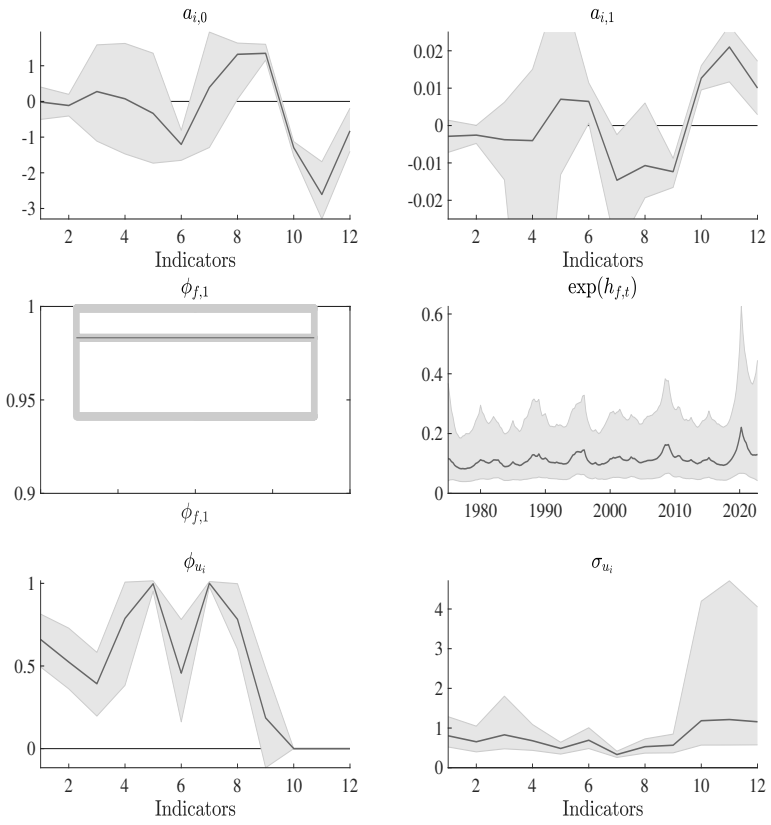

Notes: We present the posterior median estimates accompanied by 90% credible intervals. The numerical assignment for each indicator aligns with the sequential order in which the indicators are displayed in Panel (A) of Figure 1.

Figure A-2: Posterior estimates: Factor loadings and volatilities for idiosyncratic error terms

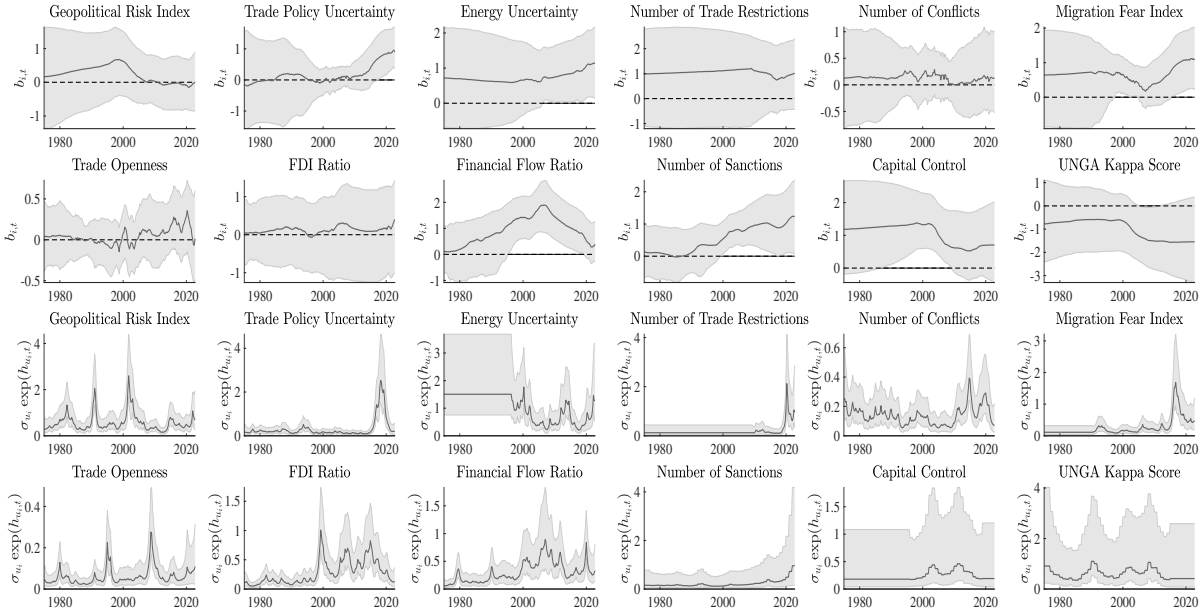

Notes: We present the posterior median estimates accompanied by 90% credible intervals.

C.2 Descriptive statistics of countries

Table A-2: List of countries

Category	Countries
AEs (34 countries)	Australia, Austria, Belgium, Canada, Switzerland, Cyprus, Czechia, Germany, Denmark, Spain, Estonia, Finland, France, U.K., Greece, Hong Kong, Ireland, Israel, Italy, Japan, South Korea, Lithuania, Luxembourg, Latvia, Malta, Netherlands, Norway, New Zealand, Portugal, Singapore, Slovakia, Slovenia, Sweden, USA
EMs (26 countries)	Argentina, Bulgaria, Brazil, Chile, Colombia, Costa Rica, Ecuador, Croatia, Hungary, Indonesia, Jamaica, Jordan, Kazakhstan, Mexico, North Macedonia, Philippines, Poland, Romania, Russia, Saudi Arabia, El Salvador, Serbia, Thailand, Turkey, Ukraine, South Africa

Notes: Country classification follows the IMF WEO.

Table A-3: Descriptive statistics of countries

Variable	N. of observations	Mean	Median	Std. Dev.	10th percentile	90th percentile
All countries						
GDP per capita (1,000 PPP$)	5,837	32.1	30.4	19.2	10.6	53.5
GDP growth per capita (%)	5,958	2.2	2.3	5.3	-3.0	7.7
Exports share (% of GDP)	6,019	48.3	37.3	38.2	19.3	83.2
Imports share (% of GDP)	6,019	47.9	37.5	34.4	20.4	79.6
Trade share (% of GDP)	6,019	96.2	74.6	72.2	40.1	161.2
Currency peg (1 for peg)	6,025	0.25	0	0.43	0	1
AEs						
GDP per capita (1,000 PPP$)	3,583	42.4	40.2	17.0	26.1	58.8
GDP growth per capita (%)	3,735	2.1	2.1	4.7	-2.5	7.1
Exports share (% of GDP)	3,765	56.2	40.4	44.9	20.4	122.2
Imports share (% of GDP)	3,765	53.6	38.7	40.3	21.1	114.3
Trade share (% of GDP)	3,765	109.9	79.9	85.1	41.9	240.1
Currency peg (1 for peg)	3,765	0.22	0	0.41	0	1
EMs						
GDP per capita (1,000 PPP$)	2,254	15.8	14.5	7.6	8.2	25.0
GDP growth per capita (%)	2,223	2.4	3.0	6.1	-3.8	8.3
Exports share (% of GDP)	2,254	34.9	32.1	15.3	18.1	54.3
Imports share (% of GDP)	2,254	38.3	34.6	17.3	19.0	65.0
Trade share (% of GDP)	2,254	73.2	67.7	31.3	37.5	118.7
Currency peg (1 for peg)	2,260	0.30	0	0.46	0	1

Notes: Pooled sample during 1986 to 2019. Currency peg is an indicator variable that takes zero for the floating exchange rate regime and one otherwise, according to the IMF Annual Report on Exchange Arrangements and Exchange Restrictions (AREAER).

C.3 Robustness checks

C.3.1 Alternative selection of indicators: Replicating the SVAR results

Figure A-3: Sensitivity to the choice of indicators in factor estimation

(A) Core 7 indicators (Trade Openness, FDI, Financial flows, Sanctions, GRI, TPU, Conflicts)

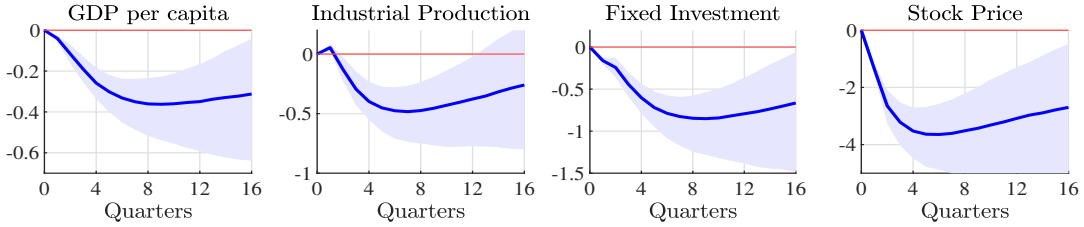

(B) All indicators in (A) & Trade Restrictions & Migration Fear Index

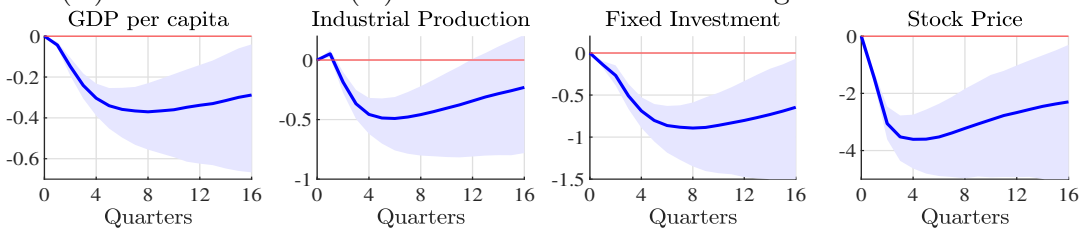

(C) All indicators in (B) & Energy Uncertainty

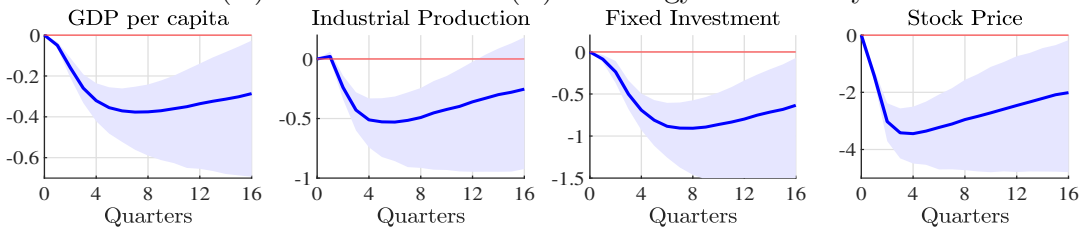

(D) All indicators in (B) & Capital Control

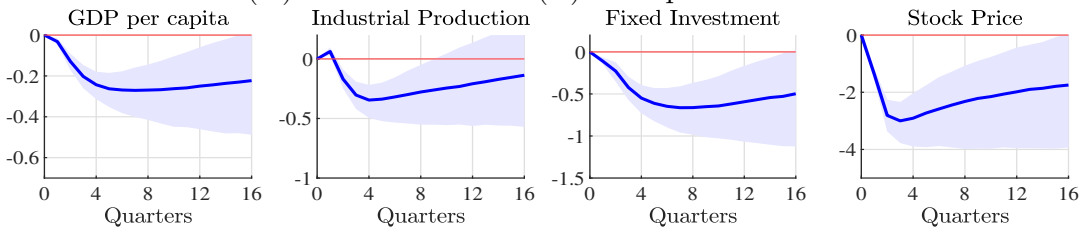

(E) All indicators in (B) & Energy Uncertainty & Capital Control

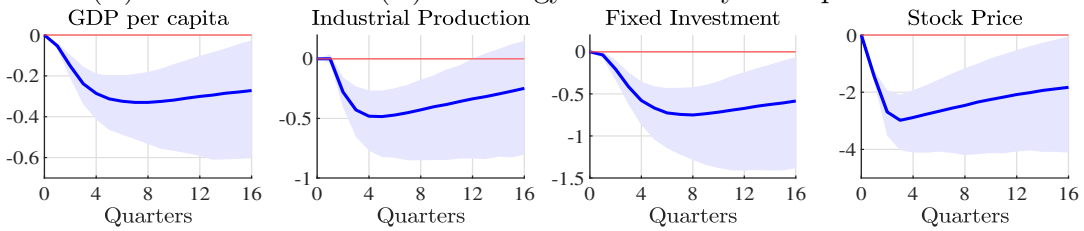

Notes: Sample of AEs and EMs. Percent responses to a 1 S.D. shock to the factor. Shaded areas indicate the 90 percentiles. The Core 7 indicators are available on a quarterly basis throughout the entire sample period.

C.3.2 Alternative prior choices: Replicating the SVAR results

Figure A-4: Sensitivity to the prior specification of factor estimation

(A) Priors 1: $\sigma^2_{b_i} \sim IG\left(1, \frac{1}{10}\right), \quad \sigma^2_{u_i} \sim IG\left(1, 1\right), \quad \sigma^2_{h_f}, \sigma^2_{h_i} \sim IG\left(1, 1\right)$

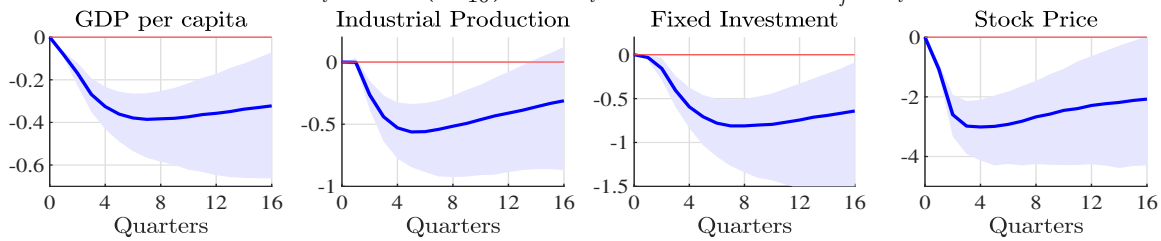

(B) Priors 2: $\sigma^2_{b_i} \sim IG\left(10, 1\right), \quad \sigma^2_{u_i} \sim IG\left(10, 10\right), \quad \sigma^2_{h_f}, \sigma^2_{h_i} \sim IG\left(10, 10\right)$

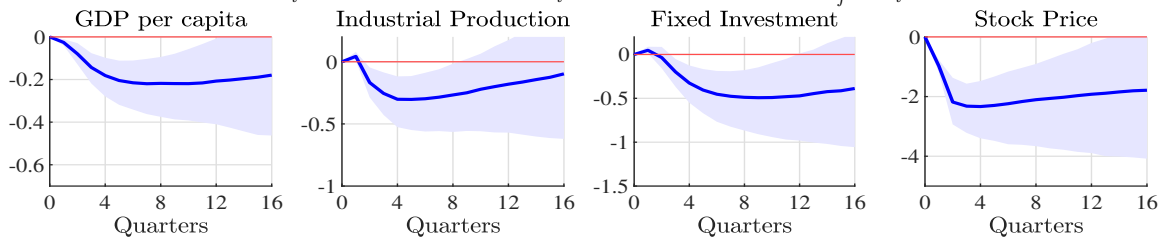

(C) Priors 3: $\sigma^2_{b_i} \sim IG\left(10, \frac{1}{10}\right), \quad \sigma^2_{u_i} \sim IG\left(1, 2\right), \quad \sigma^2_{h_f}, \sigma^2_{h_i} \sim IG\left(10, 1\right)$

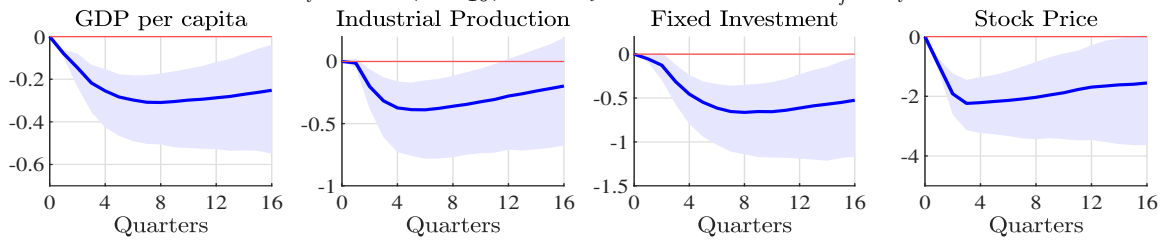

(D) Priors 4: $\sigma^2_{b_i} \sim IG\left(10, \frac{1}{10}\right), \quad \sigma^2_{u_i} \sim IG\left(1, \frac{1}{2}\right), \quad \sigma^2_{h_f}, \sigma^2_{h_i} \sim IG\left(10, 1\right)$

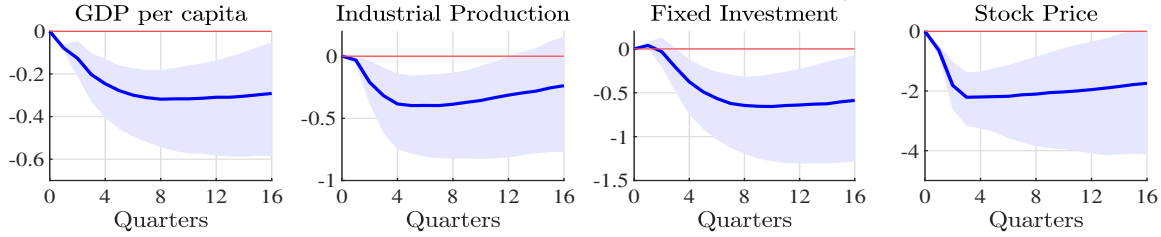

(E) Priors 5: Constant loading case $b_i \sim N\left(1, \frac{1}{2}\right)$

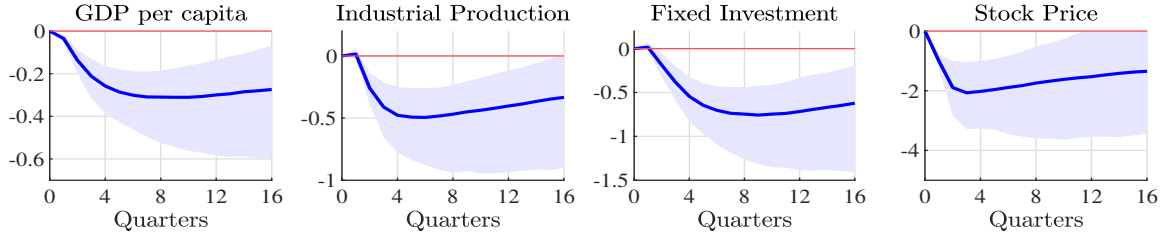

Notes: Sample of AEs and EMs. Percent responses to a 1 S.D. shock to the factor. Shaded areas indicate the 90 percentiles. Unless specified otherwise, we adhere to the previously discussed priors for the remaining parameters.

C.3.3 Using the Trade Openness instead: Replicating the SVAR results

Figure A-5: Sensitivity to replacing the fragmentation index with the Trade Openness

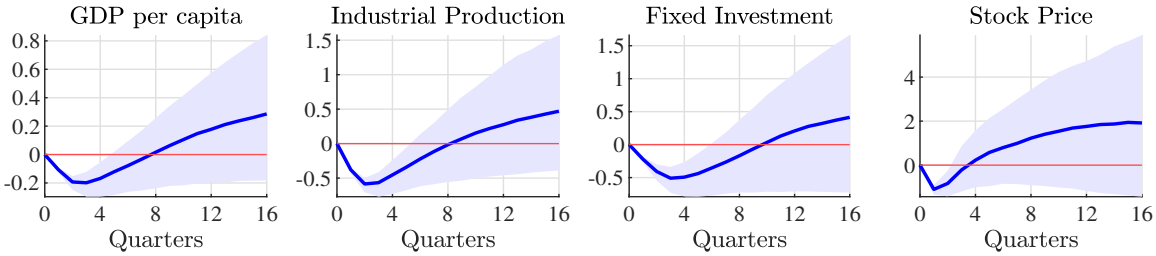

Notes: The fragmentation index is replaced with the trade share in the SVAR. Sample of AEs and EMs. Percent responses to a 1 S.D. shock to each indicator. The sign of the responses is flipped. Shaded areas indicate the 90 percentiles.

C.3.4 Alternative identification schemes: Replicating the LP results

Figure A-6: Sensitivity to alternative identification schemes

(A) Identified through differencing

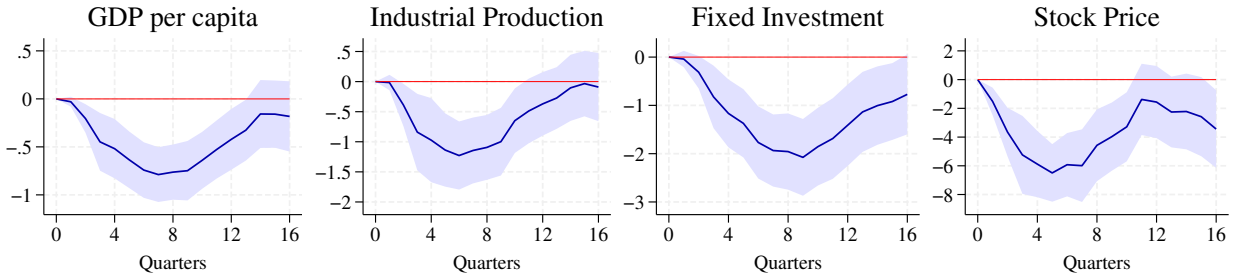

(B) Identified through Cholesky decomposition

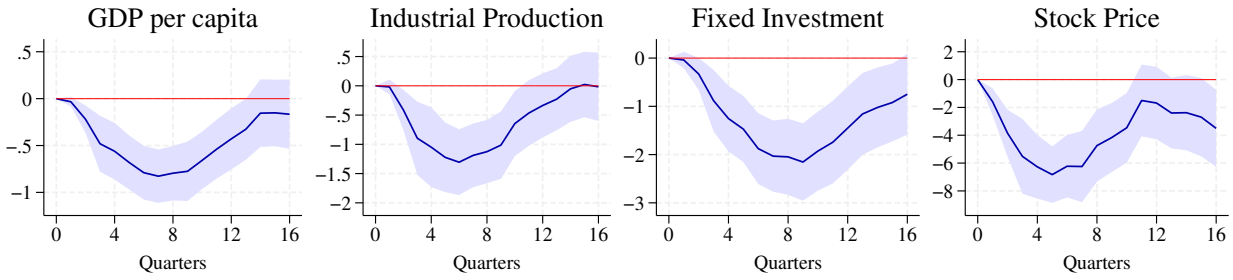

Notes: Sample of AEs and EMs. Percent responses to a 1 S.D. shock to the factor. Shaded areas indicate the 90 percentiles. In Panel (A), the first difference of the factor is used as a shock. In Panel (B), a global VAR with the first seven variables of the baseline panel VAR is run with the sample period of 1986:Q2 to 2022Q4, and the fragmentation shock is identified through the Cholesky decomposition.